

The Electronic Influence of Ring Substituents and *Ansa* Bridges in Zirconocene Complexes as Probed by Infrared Spectroscopic, Electrochemical, and Computational Studies

Cary E. Zachmanoglou,[†] Arefa Docrat,[†] Brian M. Bridgewater,[†] Gerard Parkin,^{*,†} Christopher G. Brandow,[‡] John E. Bercaw,^{*,‡} Christian N. Jardine,[§] Mark Lyall,[§] Jennifer C. Green,^{*,§} and Jerome B. Keister^{*,||}

Contribution from the Department of Chemistry, Columbia University, New York, New York 10027, Arnold and Mabel Beckman Laboratories of Chemical Synthesis, California Institute of Technology, Pasadena, California 91125, Inorganic Chemistry Laboratory, South Parks Road, Oxford, OX1 3QR, UK, and Department of Chemistry, University at Buffalo, State University of New York, Buffalo, New York 14260

Received February 15, 2002

Abstract: The electronic influence of unbridged and *ansa*-bridged ring substituents on a zirconocene center has been studied by means of IR spectroscopic, electrochemical, and computational methods. With respect to IR spectroscopy, the average of the symmetric and asymmetric stretches ($\nu_{\text{CO(av)}}$) of a large series of dicarbonyl complexes $(\text{Cp}^R)_2\text{Zr}(\text{CO})_2$ has been used as a probe of the electronic influence of a cyclopentadienyl ring substituent. For unbridged substituents (Me, Et, Prⁱ, Bu^t, SiMe₃), $\nu_{\text{CO(av)}}$ on a per substituent basis correlates well with Hammett σ_{meta} parameters, thereby indicating that the influence of these substituents is via a simple inductive effect. In contrast, the reduction potentials (E°) of the corresponding dichloride complexes $(\text{Cp}^R)_2\text{ZrCl}_2$ do not correlate well with Hammett σ_{meta} parameters, thereby suggesting that factors other than the substituent inductive effect also influence E° . *Ansa* bridges with single-atom linkers, for example [Me₂C] and [Me₂Si], exert a net electron-withdrawing effect, but the effect is diminished upon increasing the length of the bridge. Indeed, with a linker comprising a three-carbon chain, the [CH₂CH₂CH₂] *ansa* bridge becomes electron-donating. In contrast to the electron-withdrawing effect observed for a single [Me₂Si] *ansa* bridge, a pair of vicinal [Me₂Si] *ansa* bridges exerts an electron-donating effect relative to that from the single bridge. DFT calculations demonstrate that the electron-withdrawing effect of the [Me₂C] and [Me₂Si] *ansa*-bridges is due to stabilization of the cyclopentadienyl ligand acceptor orbital, which subsequently enhances back-donation from the metal. The calculations also indicate that the electron-donating effect of two vicinal [Me₂Si] *ansa* bridges, relative to that of a single bridge, is a result of it enforcing a ligand conformation that reduces back-donation from the metal.

Introduction

Zirconocene complexes have attracted considerable attention due to their applications as catalyst precursors for olefin polymerization¹ and as reagents for organic synthesis.² The

usefulness of the zirconocene system may in part be attributed to the facile incorporation of a variety of substituents on the cyclopentadienyl rings which allows for the chemistry to be modulated in significant ways. A particularly important class of ring substituents is one that links the two cyclopentadienyl groups together, that is, a so-called *ansa* bridge,³ because, among other factors, it increases the configurational stability of the metallocene fragment. Most investigations into ligand effects

* To whom correspondence should be addressed. E-mail: parkin@chem.columbia.edu.

[†] Columbia University.

[‡] California Institute of Technology.

[§] Inorganic Chemistry Laboratory, Oxford.

^{||} University at Buffalo, State University of New York.

- (1) (a) Brintzinger, H. H.; Fischer, D.; Mülhaupt, R.; Rieger, B.; Waymouth, R. M. *Angew. Chem., Int. Ed. Engl.* **1995**, *34*, 1143–1170. (b) Grubbs, R. H.; Coates, G. W. *Acc. Chem. Res.* **1996**, *29*, 85–93. (c) Möhring, P. C.; Coville, N. J. *J. Organomet. Chem.* **1994**, *479*, 1–29. (d) Kaminsky, W.; Arndt, M. *Adv. Polym. Sci.* **1997**, *127*, 143–187. (e) Kaminsky, W. *J. Chem. Soc., Dalton Trans.* **1998**, 1413–1418. (f) Olabisi, O.; Atiqullah, M.; Kaminsky, W. *J. Macromol. Sci., Rev. Macromol. Chem. Phys.* **1997**, *C37*, 519–554. (g) Green, J. C. *Chem. Soc. Rev.* **1998**, *27*, 263–271. (h) Ivchenko P. V., Nifantev I. E. *Zh. Org. Khim.* **1998**, *34*, 9–38. (i) Ewen, J. A. *Sci. Am.* **1997**, *276*, 86–91.
- (2) (a) Negishi, E.; Takahashi, T. *Synthesis* **1988**, 1–19. (b) Buchwald, S. L.; Broene, R. D. In *Comprehensive Organometallic Chemistry II*; Abel, E. W., Stone, F. G. A., Wilkinson, G., Eds.; Pergamon: Elmsford, NY, Vol. 12, pp 771–784. (c) Hoveyda, A. H.; Morken, J. P. *Angew. Chem., Int. Ed. Engl.* **1996**, *35*, 1262–1284.

- (3) The concept of bridged metallocene derivatives dates back to 1956 with Nesmeyanov's proposal for bridged ferrocene derivatives.³ The first example of such a complex, namely the ferrocene derivative, $[\{(\text{CH}_2)_2\text{C}(\text{O})\}(\text{C}_5\text{H}_4)_2]\text{Fe}$, was described shortly thereafter by Rinehart and Curby in 1957,^b and the Latin term *ansa* (meaning bent handle, attached at both ends) was first applied to metallocene chemistry by Lüttringhaus and Kullick in 1958 for $[(\text{CH}_2)_n(\text{C}_5\text{H}_4)_2]\text{Fe}$ ($n = 3-5$).^{c,d} Bent *ansa* metallocene chemistry has its origins with Katz's synthesis of $[\text{H}_2\text{C}(\text{C}_5\text{H}_4)_2]\text{TiCl}_2$ ^e and the first of Brintzinger's epic contributions in 1979.^f (a) Nesmeyanov, A. N.; Volkenau, N. A.; Vilchevskaya, V. D. *Dokl. Akad. Nauk S.S.S.R.* **1956**, *111*, 362–364. (b) Rinehart, K. L.; Curby, R. J., Jr. *J. Am. Chem. Soc.* **1957**, *79*, 3290–3291. (c) Lüttringhaus A.; Kullick, W. *Angew. Chem.* **1958**, *70*, 438. (d) Lüttringhaus A.; Kullick, W. *Makromol. Chem.* **1961**, *44-46*, 669–681. (e) Katz, T. J.; Acton, N. *Tetrahedron Lett.* **1970**, 2497–2499. (f) Smith, J. A.; von Seyerl, J.; Huttner, G.; Brintzinger, H. H. *J. Organomet. Chem.* **1979**, *173*, 175–185.

on the reactivity of zirconocene complexes have focused on steric effects, with relatively few studies having addressed electronic effects.⁴ In this paper, we describe a series of structural, spectroscopic, electrochemical, and theoretical studies to evaluate the electronic influence of various ring substituents, including *ansa* bridges, on the metal center of zirconocene complexes.

The incorporation of substituents on cyclopentadienyl rings may have profound consequences.⁵ For example, simple zirconocene dihydride complexes of the type $[(Cp^R)_2ZrH_2]_n$,⁶ with a single alkyl substituent (e.g., R = Me, Prⁱ, Bu^t) on each of the cyclopentadienyl groups, are typically dimeric or oligomeric, and isolation of monomeric derivatives requires the presence of several substituents, for example, Cp^*ZrH_2 , $Cp^*(Cp^{Me_4})ZrH_2$, $Cp^*(Cp^{1,2,4-Me_3})ZrH_2$, $Cp^*(Cp^{1,3-Bu^t})ZrH_2$, and $(Cp^{1,3-Bu^t})_2ZrH_2$.⁷ Of more commercial relevance, cyclopentadienyl ring substituents strongly influence the activity and stereospecificity of zirconocene olefin polymerization catalysts. The influence is, however, complex.^{5,8} For example, the order of ethylene polymerization activity for a series of $(Cp^R)_2ZrCl_2$ complexes depends on the choice of alkylalumoxane cocatalyst,^{5,9,10} while the trends in propylene polymerization activity for multiply substituted $(Cp^R)_2ZrCl_2$ /methylalumoxane catalysts indicate that the number of substituents, their sizes, locations, and electron-donating abilities are all likely to be important.^{5,11}

An *ansa*-bridged substituent, however, exerts an additional effect due to the constraints associated with the natural bond angle preferences of the bridging atoms. The influence of an *ansa* bridge may be significant, as illustrated by the effect of a $[Me_2Si]$ bridge on the chemistry of permethylzirconocene complexes,¹² viz, (i) $Cp^*_2ZrMe_2$ reacts with H_2 in benzene to give $Cp^*_2ZrH_2$, whereas $[Me_2Si(C_5Me_4)_2]ZrMe_2$ gives the phenyl-hydride derivative $[Me_2Si(C_5Me_4)_2]Zr(Ph)H$, (ii) THF and PMe_3 bind more strongly to the zirconium center of $\{[Me_2Si(C_5Me_4)_2]ZrH_2\}$ than to that of $Cp^*_2ZrH_2$, and (iii) $Cp^*_2ZrH_2$ is a monomer, whereas its *ansa* counterpart is a dimer, $\{[Me_2Si(C_5Me_4)_2]Zr(H)(\mu-H)\}_2$. It is also important to note that the reactivity of a metallocene system is further modulated upon incorporation of a second *ansa* bridge. For example, whereas hydrogenation of the singly bridged *ansa* complexes *meso*- $[Me_2Si(C_5H_3-3-Bu^t)_2]ZrMe_2$ and *rac*- $[Me_2Si(C_5H_2-2-TMS-4-Bu^t)_2]ZrMe_2$ is facile at room temperature, the doubly bridged complexes $[(Me_2Si)_2(C_5H_3)_2]ZrMe_2$, $[(Me_2Si)_2(C_5H-3,5-Pr^i)_2(C_5H_2-4-Pr^i)]ZrMe_2$, and $[(Me_2Si)_2(C_5H-3,5-Pr^i)_2(C_5H_2-4-CHMeEt)]ZrMe_2$ are only hydrogenated under forcing con-

ditions.¹³ *Ansa* bridges also influence olefin polymerization activity. Thus, with respect to ethylene polymerization by $(Cp^R)_2ZrCl_2$ /methylalumoxane, a $[Me_2Si]$ bridge increases the activity, whereas a $[Me_2C]$ bridge almost completely inhibits the activity.¹⁴ In contrast to the activating effect of a single $[Me_2Si]$ bridge, a pair of vicinal $[Me_2Si]$ *ansa* bridges exerts an inhibitory effect with respect to olefin polymerization. For example, a catalyst composed of a mixture of $[(Me_2Si)_2(C_5H-3,4-Me_2)_2]ZrCl_2$ and methylalumoxane shows little activity,^{15,16} in contrast to the high activity of singly bridged counterparts. To evaluate the origin of the differences between the *ansa* and nonbridged systems, we have performed a variety of studies on zirconocene derivatives to evaluate the electronic influence of *ansa* substituents. At the outset, it should be emphasized that the electronic influence of certain *ansa* bridges has been previously considered in the literature. Some of these results are, however, contradictory. For example, some studies have proposed that a $[Me_2Si]$ *ansa* bridge makes a zirconocene center more electron-rich,^{17,18} whereas other studies have suggested that the electron density is reduced.^{19–21} To address the electronic influence of *ansa* bridges in more detail, we have experimentally examined (i) the electrochemistry of zirconocene dichlorides and (ii) the IR spectroscopy of zirconocene dicarbonyls, the results of which demonstrate that *inferences* pertaining to the relative electron-donating properties of the ring substituents are influenced by the method used to probe the effect. Finally, computational studies on these complexes provide a theoretical foundation for the experimental results.

Results and Discussion

The influence of an *ansa* bridge on the reactivity and physical properties of a metallocene complex is expected to be closely linked to its structure. As such, it is appropriate that we first describe the structural consequences of incorporating an *ansa* bridge. The section on the structural consequences of substituents is followed by a discussion of the influence of both nonbridged and *ansa*-bridged substituents on the electronic properties of a zirconocene center. Finally, we conclude with a computational analysis of the results.

1. Structures of Zirconocene Complexes with Single and Double *Ansa* Bridges. Simple alkyl substituents on a cyclopentadienyl ring may, in principle, influence the electronic

- (4) See, for example: Janiak, C. In *Metallocenes: Synthesis, Reactivity, Applications*; Togni, A., Halterman, R., Eds.; Wiley-VCH: Weinheim, Germany, 1998; Vol. 2, pp 576–577.
- (5) For a review of the influence of ring substituents on Group 4 metallocene Ziegler–Natta Catalysts, see: Möhring, P. C.; Coville, N. J. *J. Organomet. Chem.* **1994**, *479*, 1–29.
- (6) For simplicity, the abbreviation (Cp^R) is used generally to refer to any substituted cyclopentadienyl ligand, including multiply substituted derivatives.
- (7) Chirik, P. J.; Day, M. W.; Bercaw, J. E. *Organometallics* **1999**, *18*, 1873–1881.
- (8) Contributing to this complexity of cyclopentadienyl substituents and catalyst “activity” is the fact that the fraction of catalytically active zirconocene centers during polymerization is generally low and strongly dependent on the nature of the substituents.
- (9) Möhring, P.; Coville, N. J. *J. Mol. Catal.* **1992**, *77*, 41–50.
- (10) The trend was rationalized in terms of the activity being promoted by both decreased ligand size and increased electron-donating ability, but being dominated by the electronic component.
- (11) Harada, M.; Mise, T.; Miya, S.; Yamazaki, H. Eur. Pat. Appl. EP0283739, 1988.
- (12) Lee, H.; Desrosiers, P. J.; Guzei, I.; Rheingold, A. L.; Parkin, G. *J. Am. Chem. Soc.* **1998**, *120*, 3255–3256.

- (13) Chirik, P. J.; Henling, L. M.; Bercaw, J. E. *Organometallics* **2001**, *20*, 534–544.
- (14) Specific values [10^3 kg PE/(mol Zr·h·atm C_2H_4)]: $[Me_2Si(C_5H_4)_2]ZrCl_2$ (18.4), Cp_2ZrCl_2 (16.6), $[Me_2C(C_5H_4)_2]ZrCl_2$ (0.03). See: Quijada, R.; DuPont, J.; Correa Silveira, D.; Lacerda Miranda, M. S.; Scipioni, R. B. *Macromol. Rapid Commun.* **1995**, *16*, 357–362.
- (15) Mengele, W.; Diebold, J.; Troll, C.; Röhl, W.; Brintzinger, H. H. *Organometallics* **1993**, *12*, 1931–1935.
- (16) Furthermore, it should be noted that the activity that was observed was attributed to degradation of the doubly bridged complex to a singly bridged species.
- (17) Gassman, P. G.; Deck, P. A.; Winter, C. H.; Dobbs, D. A.; Cao, D. H. *Organometallics* **1992**, *11*, 959–960.
- (18) (a) Beck, S.; Brintzinger, H. H. *Inorg. Chim. Acta* **1998**, *270*, 376–381. (b) Wieser, U.; Babushkin, D.; Brintzinger, H.-H. *Organometallics* **2002**, *21*, 920–923.
- (19) Siedle, A. R.; Newmark, R. A.; Lamanna, W. M.; Schroepfer, J. N. *Polyhedron* **1990**, *9*, 301–308.
- (20) Bajgur, C. S.; Tikkanen, W. R.; Petersen, J. L. *Inorg. Chem.* **1985**, *24*, 2539–2546.
- (21) (a) Alameddini, N. G.; Ryan, M. F.; Eyler, J. R.; Siedle, A. R.; Richardson, D. E., *Organometallics* **1995**, *14*, 5005–5007. (b) Richardson, D. E.; Alameddini, N. G.; Ryan, M. F.; Hayes, T.; Eyler, J. R.; Siedle, A. R. *J. Am. Chem. Soc.* **1996**, *118*, 11244–11253. (c) Richardson, D. E. ACS Symposium Series; American Chemical Society: Washington, 1997; Vol. 253, pp 79–90.

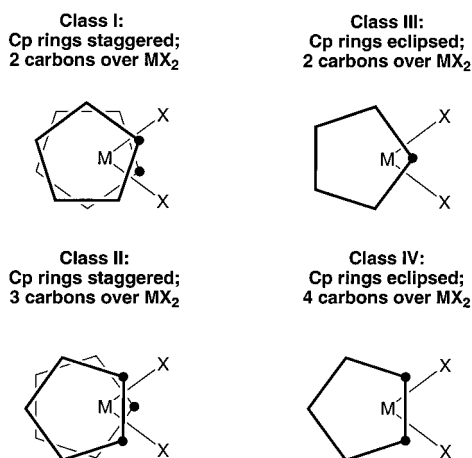


Figure 1. Classification of Cp_2MX_2 conformations.

properties of a metal center not only by exerting an inductive effect, but also by displacing the cyclopentadienyl rings from their natural positions in the parent system, $[\text{Cp}_2\text{MX}_n]$. In this regard, it is well established that simple alkyl substituents influence the conformational preferences of cyclopentadienyl ligands in bent metallocene complexes of the type $(\text{Cp}^R)_2\text{MX}_2$,²² which may be considered to belong to four idealized classes (Figure 1).²³ The specific conformation adopted is a compromise that minimizes steric interactions between (i) the cyclopentadienyl substituents at the narrow rear of the metallocene wedge and (ii) the cyclopentadienyl substituents and the X groups attached to the metal. Cyclopentadienyl ring substituents also influence the $\text{Cp}_{\text{cent}}-\text{M}-\text{Cp}_{\text{cent}}$ angle and the coordination gap,²⁴ while *ansa*-bridged substituents exert an additional influence due to constraints resulting from the geometrical preferences of the bridge itself.

The principal geometrical changes that result upon incorporation of various *ansa* bridges can be illustrated by comparison of the structures of selected zirconocene complexes.^{25,26} However, that of the simplest *ansa*-zirconocene complex, that is, methylene-bridged $[\text{H}_2\text{C}(\text{C}_5\text{H}_4)_2]\text{ZrCl}_2$, is absent from the literature. This absence is rather surprising, considering that a very large number of zirconocene complexes have been synthesized and structurally characterized; furthermore, the titanium analogue $[\text{H}_2\text{C}(\text{C}_5\text{H}_4)_2]\text{TiCl}_2$ was the first bent *ansa*-metallocene to be synthesized more than 30 years ago.^{3e} The dichloride $[\text{H}_2\text{C}(\text{C}_5\text{H}_4)_2]\text{ZrCl}_2$ may, nevertheless, be synthesized by treatment of $[\text{H}_2\text{C}(\text{C}_5\text{H}_4)_2]\text{Li}_2$ with ZrCl_4 at -78°C , followed by warming to room temperature, from which the diiodide may be obtained by metathesis with Me_3SiI .²⁷ The structures of these parent methylene-bridged complexes, $[\text{H}_2\text{C}(\text{C}_5\text{H}_4)_2]\text{ZrCl}_2$ and $[\text{H}_2\text{C}(\text{C}_5\text{H}_4)_2]\text{ZrI}_2$, together with that of the ethylene-bridged

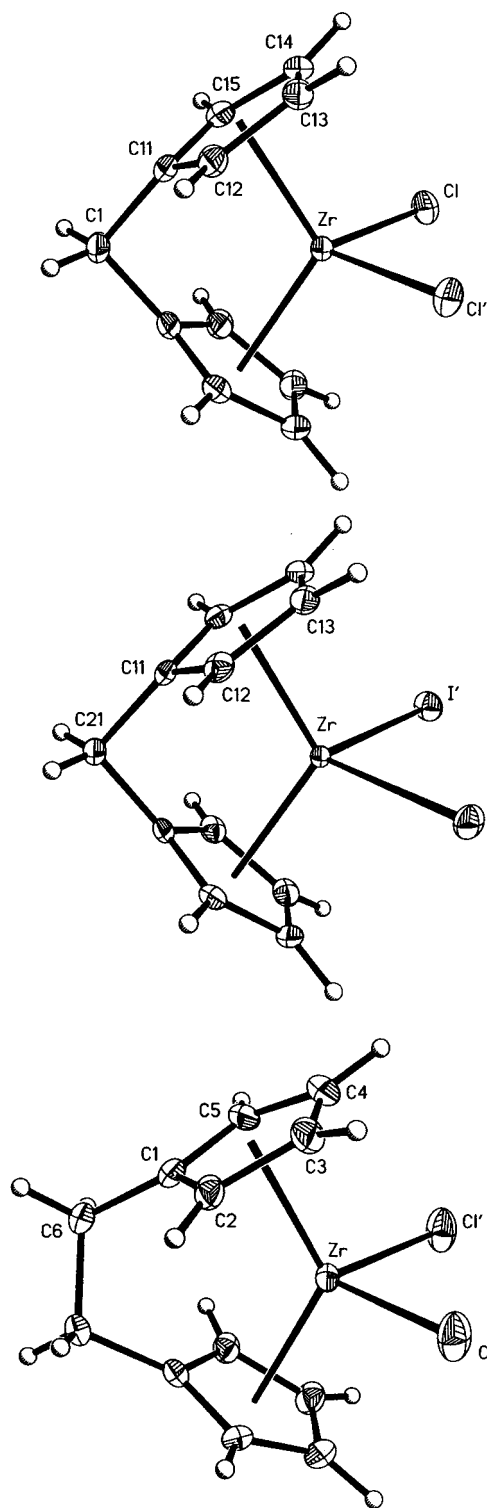


Figure 2. Molecular structures of $[\text{H}_2\text{C}(\text{C}_5\text{H}_4)_2]\text{ZrCl}_2$, $[\text{H}_2\text{C}(\text{C}_5\text{H}_4)_2]\text{ZrI}_2$, and $[(\text{CH}_2\text{CH}_2)(\text{C}_5\text{H}_4)_2]\text{ZrCl}_2$ (only one conformation of the bridge is shown).

derivative $[(\text{CH}_2\text{CH}_2)(\text{C}_5\text{H}_4)_2]\text{ZrCl}_2$ (Figure 2), have been determined to complement the existing structural data on more heavily substituted *ansa*-zirconocene derivatives.²⁸ Selected metrical data for these and other complexes are presented in Table 1.

(22) See, for example: Krüger, C.; Nolte, M.; Erker, G.; Thiele, S. Z. *Naturforsch. (B)* **1992**, *47*, 995–999.

(23) If there are substituents on the rings, it is possible to construct many additional conformations for each of these four classes. See: Trnka, T. M.; Bonanno, J. B.; Bridgewater, B. M.; Parkin, G. *Organometallics* **2001**, *20*, 3255–3264.

(24) Hortman, K.; Brintzinger, H.-H. *New J. Chem.* **1992**, *16*, 51–55.

(25) Shaltout, R. M.; Corey, J. Y.; Rath, N. P. *J. Organomet. Chem.* **1995**, *503*, 205–212.

(26) For recent molecular mechanics calculations concerned with the geometries of $[\text{Me}_2\text{Si}]$ *ansa*-metallocenes, see: Brintzinger, H.-H.; Prosenc, M.-H.; Schaper, F.; Weeber, A.; Wieser, U. *J. Mol. Struct.* **1999**, *485–486*, 409–419.

(27) For the use of Me_3SiI as a metathesis reagent in metallocene chemistry, see: Rabinovich, D.; Bott, S. G.; Nielsen, J. B.; Abney, K. D. *Inorg. Chim. Acta* **1998**, *274*, 232–235.

(28) Under comparable conditions, the ethylene polymerization catalytic activity follows the sequence: $[\text{H}_2\text{C}(\text{C}_5\text{H}_4)_2]\text{ZrCl}_2 < \text{Cp}_2\text{ZrCl}_2 < [(\text{CH}_2\text{CH}_2)(\text{C}_5\text{H}_4)_2]\text{ZrCl}_2$.

Table 1. Geometrical Data for Selected (Cp^R)₂ZrCl₂ Derivatives

	α /deg	β /deg	γ /deg	τ /deg	ϕ /deg	$\Delta(d_{M-C})/\text{Å}$	ref
Unbridged							
Cp ₂ ZrCl ₂	53.5	126.5	129.2	1.4	-	0.041	1
(Cp ^{Me}) ₂ ZrCl ₂	53.6	126.4	133.3	3.45	-	0.118	2
Cp ^{Et} ₂ ZrCl ₂	43.7	136.3	130.9	-2.7	-	0.067	3
(Cp ^{Me} ^{Et}) ₂ ZrCl ₂	43.8	136.2	137.0	0.4	-	0.036	4
Single Bridges							
[H ₂ C(C ₅ H ₄) ₂]ZrCl ₂	70.0	110.0	116.4	3.2	16.3	0.104	this work
[H ₂ C(C ₃ H ₄) ₂]ZrCl ₂	70.8	109.2	116.6	3.7	15.7	0.114	this work
[Me ₂ C(C ₅ H ₄) ₂]ZrCl ₂	71.4	108.6	116.6	4.0	14.9	0.118	5,6
[(CH ₂ CH ₂)(C ₅ H ₄) ₂]ZrCl ₂	56.4	123.6	125.8	1.1	4.3	0.053	this work
[(Me ₂ CMe ₂ C)(C ₅ H ₄) ₂]-ZrCl ₂	57.4	122.6	125.0	1.2	3.0	0.048	7
[(CH ₂ CH ₂)(C ₅ Me ₄) ₂]-ZrCl ₂	57.7	122.3	127.7	2.6	1.3	0.095	8
[(CH ₂ CH ₂ CH ₂)(C ₅ H ₄) ₂]-ZrCl ₂	50.2	129.8	129.6	-0.1	7.0	0.027	8
[Me ₂ Si(C ₅ H ₄) ₂]ZrCl ₂	60.1	119.9	125.4	2.8	16.6	0.074	10
[Me ₂ Si(C ₅ Me ₄) ₂]ZrCl ₂	60.8	119.2	128.6	4.7	17.8	0.149	6
[(Me ₂ SiMe ₂ Si)(C ₅ H ₄) ₂]-ZrCl ₂	51.2	128.8	130.9	1.05	0.5	0.031	11
[(Me ₂ SiMe ₂ Si)(C ₅ Me ₄) ₂]-ZrCl ₂	50.3	129.7	136.1	3.2	-13.4	0.095	12
[(Me ₂ SiOMe ₂ Si)(C ₅ H ₄) ₂]-ZrCl ₂	51.1	128.9	130.8	0.95	5.1	0.036	13
Double Bridges							
{[(CH ₂ CH ₂) ₂](C ₅ H ₃) ₂ }-ZrCl ₂	62.5	117.5	120.0	1.25	1.7	0.052	14
[(Me ₂ Si) ₂ (C ₅ H ₃) ₂]ZrCl ₂	69.6	110.4	120.6	5.1	19.6	0.157	15

(1) Corey, J. Y.; Zhu, X.-H.; Brammer, L.; Rath, N. P. *Acta Crystallogr.* **1995**, *C51*, 565–567. (2) Janiak, C.; Versteeg, U.; Lange, K. C. H.; Weimann, R.; Hahn, E. *J. Organomet. Chem.* **1995**, *501*, 219–234. (3) CSD reference code GEJPEQ. (4) Kurz, S.; Heyhawkins, E. *Z. Kristallogr.* **1993**, *205*, 61–67. (5) Shaltout, R. M.; Corey, J. Y.; Rath, N. P. *J. Organomet. Chem.* **1995**, *503*, 205–212. (6) Koch, T.; Blaurock, S.; Somoza, F. B., Jr.; Voight, A.; Kirmse, R.; Hey-Hawkins, E. *Organometallics* **2000**, *19*, 2556–2563. (7) Bühl, M.; Hopp, G.; von Philipsborn, W.; Beck, S.; Prosenec, M.-H.; Rief, U.; Brintzinger, H.-H. *Organometallics* **1996**, *15*, 778–785. (8) Wochner, P.; Zsolnai, L.; Huttner, G.; Brintzinger, H. H. *J. Organomet. Chem.* **1985**, *288*, 69–77. (9) Saldarriaga-Molina, C. H.; Clearfield, A.; Bernal, I. *J. Organomet. Chem.* **1974**, *80*, 79–90. (10) Bajgur, C. S.; Tikkanen, W. R.; Petersen, J. L. *Inorg. Chem.* **1985**, *24*, 2539–2546. (11) Thiele, K. H.; Schliessburg, C.; Baumeister, K.; Hassler, K. Z. *Anorg. Allg. Chem.* **1996**, *622*, 1806–1810. (12) Zachmanoglou, C. E.; Parkin, G. Unpublished results. (13) Ciruelos, S.; Cuenca, T.; Gómez-Sal, P.; Manzanero, A.; Royo, P. *Organometallics* **1995**, *14*, 177–185. (14) (a) Dorer, B.; Prosenec, M.-H.; Rief, U.; Brintzinger, H. H. *Organometallics* **1994**, *13*, 3868–3872. (b) Hafner, K.; Mink, C.; Lindner, H. *J. Angew. Chem., Int. Ed. Engl.* **1994**, *33*, 1479–1480. (15) Cano, A.; Cuenca, T.; Gómez-Sal, P.; Royo, E.; Royo, P. *Organometallics* **1994**, *13*, 1688–1694.

For a bent metallocene with idealized C_{2v} geometry, the structure may be defined by the angular parameters illustrated in Figure 3. Unfortunately, the nomenclature pertaining to these parameters is used inconsistently in the literature so that it is necessary to state that the following convention is adopted here: α = interplanar-ring angle; β = Cp_{norm}–Cp_{norm} angle ($\alpha + \beta = 180^\circ$); γ = Cp_{cent}–M–Cp_{cent} angle; $\tau = 0.5(\gamma - \beta)$ = tilt angle (the angle between the M–Cp_{cent} vector and the ring normal);²⁹ θ = C_{ipso}–A–C_{ipso} angle, where A represents a bridging atom; and $\phi = 180^\circ - (A-C_{ipso}-Cp_{cent})$, the angle between the A–C_{ipso} vector and the Cp mean plane.^{30,31} With respect to α (or β), γ and τ , it should be noted that these angles may not all be varied independently, but are related by the expression $\alpha = 2\tau - \gamma + 180^\circ$. Thus, while the Cp_{cent}–M–Cp_{cent} angle (γ) and the tilt angle (τ) may be varied indepen-

dently of each other, variations in γ and τ also modify the inter-ring angle (α).

The geometrical consequences of incorporating an *ansa* bridge with a single-atom linker are mainly a result of the natural C_{ipso}–A–C_{ipso} angle (θ) in a fully relaxed ligand being too large to allow efficient interaction between a metal and the cyclopentadienyl rings. Thus, coordination to a transition metal requires a compromise of the bonding requirements of the metal center, the *ipso* carbon atom of the cyclopentadienyl ring, and the atoms of the *ansa* bridge, typically resulting in displacement of the cyclopentadienyl rings to a geometry in which the *ipso* carbon becomes nonplanar and the metal–Cp_{cent} vector is no longer normal to the Cp ring. Also as a compromise, both C_{ipso}–A–C_{ipso} (θ) and Cp_{cent}–M–Cp_{cent} (γ) angles are typically reduced from their natural values in an unconstrained system. With respect to Figure 3, a complication for *ansa* metallocenes resides with the fact that although such fragments are often represented as possessing a C_{2v} geometry, deviations from this geometry in which the *ansa* bridge does not lie symmetrically about the C₂ axis are well precedented, especially for bridges that involve more than one atom.³² As such, the simplistic nature of the representation of Figure 3 should be recognized. A further caveat, which applies to all bent metallocene derivatives, is that if the cyclopentadienyl rings are twisted such that they are not orthogonal to the Cp_{cent}–M–Cp_{cent} plane, the angle between the cyclopentadienyl ring planes will *not* be equal to α as projected in Figure 3.

The main structural effect of incorporating a single-atom linker is to modify the Cp_{cent}–M–Cp_{cent} (γ) angle, with the effect being greatest for the smallest bridge, [R₂C] (R = H, Me). The tilt angles (τ) also vary with the *ansa* bridge, but to a lesser degree than do the Cp_{cent}–M–Cp_{cent} (γ) angles. Nevertheless, the tilt angles, which correlate with the variation in M–C bond lengths (Δd_{M-C}), indicate that a single-atom *ansa* bridge causes a shift in coordination of the cyclopentadienyl rings towards η^3 -coordination, with the *ipso* and two neighboring carbon atoms being closer to the metal than the two distal carbons. A final noteworthy feature of an *ansa* bridge with a single-atom linker is the stabilization of an eclipsed conformation in which one vertex of each cyclopentadienyl ring points towards the rear of the metallocene wedge (Class IV, Figure 1). In the absence of an *ansa* bridge, this conformation is normally unstable because of interannular interactions between the cyclopentadienyl substituents in the rear of the wedge. This conformation also results in a central coordination site being more spacious since it is never eclipsed by a substituent.

Increasing the size of the linker allows the Cp_{cent}–M–Cp_{cent} (γ) angle to expand and approach the value in the unlinked system, as illustrated by the series: [H₂C(C₅H₄)₂]ZrCl₂ (116.4°), [(CH₂CH₂)(C₅H₄)₂]ZrCl₂ (125.8°), [(CH₂CH₂CH₂)(C₅H₄)₂]ZrCl₂ (129.6°), and Cp₂ZrCl₂ (129.2°).³³ Another effect of increasing the size of the linker is to modify the conformation of the cyclopentadienyl rings in an effort to obtain a better match for the length of the linker. However, this necessarily increases interannular nonbonded interactions at the rear of the wedge and thus is disfavored by the presence of bulky substituents

(29) Howard, C. G.; Girolami, G. S.; Wilkinson, G.; Thornton-Pett, M.; Hursthouse, M. B. *J. Am. Chem. Soc.* **1984**, *106*, 2033–2040.

(30) It should be noted that ϕ has also been referred to as a tilt angle. See, for example: Harder, S.; Lutz, M.; Straub, A. W. G. *Organometallics* **1997**, *16*, 107–113.

(31) Additional parameters for describing metallocene structures include the coordination gap aperture and obliquity angle. See ref 24.

(32) (a) Burger, P.; Hortman, K.; Brintzinger, H.-H. *Makromol. Chem., Macromol. Symp.* **1993**, *66*, 127–140. (b) Burger, P.; Diebold, J.; Gutman, S.; Hund, H.-H.; Brintzinger, H.-H. *Organometallics* **1992**, *11*, 1319–1327. (33) For comparison of the titanium complexes, [(H₂C)_n(C₅H₄)₂]TiCl₂ ($n = 1-3$), see ref 3f.

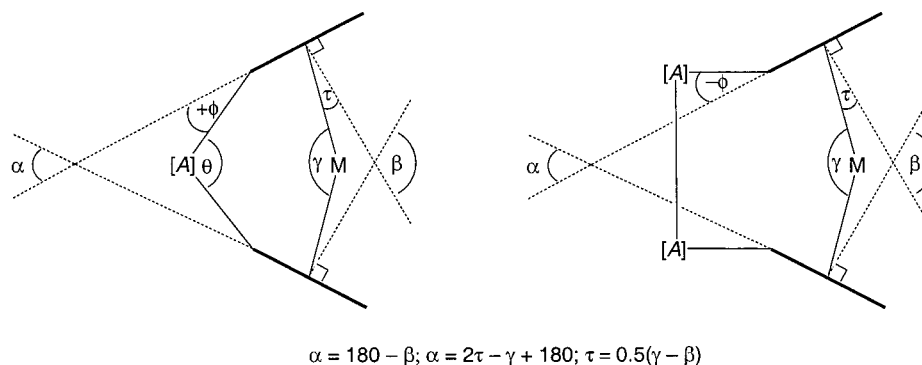


Figure 3. Parameters to define metalocene geometries, as illustrated for single- and double-atom bridges.

adjacent to the bridge. As an illustration of this effect, $[(\text{SiMe}_2\text{-SiMe}_2)(\text{C}_5\text{H}_4)_2]\text{ZrCl}_2$ ³⁴ adopts a conformation in which the $[\text{SiMe}_2\text{SiMe}_2]$ *ansa* bridge is asymmetrically displaced from the *pseudo*- C_2 axis, whereas that of $[(\text{SiMe}_2\text{SiMe}_2)(\text{C}_5\text{Me}_4)_2]\text{ZrCl}_2$ ³⁵ is symmetrically disposed, such that the complex maintains C_2 symmetry. The inability of the $[(\text{SiMe}_2\text{SiMe}_2)(\text{C}_5\text{Me}_4)_2]$ ligand to adopt a conformation in which the $[\text{SiMe}_2\text{SiMe}_2]$ bridge is displaced from the C_2 axis results in a *negative* value of ϕ at the *ipso* carbon atom, that is, the bridge is actively attempting to force the cyclopentadienyl rings to become more parallel (Figure 3). However, such closure is prevented by interactions between the ring substituents and the chloride ligands. In this regard, the $\text{Cp}_{\text{cent}}\text{-M-Cp}_{\text{cent}}$ (γ) angle for $[(\text{SiMe}_2\text{SiMe}_2)(\text{C}_5\text{Me}_4)_2]\text{ZrCl}_2$ (136.1°) is comparable to the maximum value that has been observed in the literature for methylated derivatives (138.8°), which is typically associated with bulky substituents, for example, $(\text{Cp}^{\text{Bu}_3})(\text{Cp}^{\text{Pr}_4})\text{ZrCl}_2$ (138.8°)³⁶ and $\text{Ind}^*_2\text{ZrCl}_2$ (138.3°)³⁷.

A double *ansa* bridge has a much more pronounced effect than a single bridge. For example, comparison of the structures of Cp_2ZrCl_2 , $[\text{Me}_2\text{Si}(\text{C}_5\text{H}_4)_2]\text{ZrCl}_2$ and the doubly bridged complex $[(\text{Me}_2\text{Si})_2(\text{C}_5\text{H}_3)_2]\text{ZrCl}_2$ ³⁸ demonstrates that there is a progressive opening of the metallocene wedge, as indicated by the increase in α and decrease in γ (Table 1). Correspondingly, the tilt angle (τ) increases from 1.4° for Cp_2ZrCl_2 to 2.8° for $[\text{Me}_2\text{Si}(\text{C}_5\text{H}_4)_2]\text{ZrCl}_2$, and to 5.1° for $[(\text{Me}_2\text{Si})_2(\text{C}_5\text{H}_3)_2]\text{ZrCl}_2$; this variation in tilt angle is accompanied by an increase in the variation of Zr-C bond lengths for each cyclopentadienyl ring (Table 1). The chiral derivatives $[(\text{Me}_2\text{Si})_2(\text{C}_5\text{HMe}_2)_2]\text{ZrCl}_2$ and $[(\text{Me}_2\text{Si})_2(\text{tetrahydroindenediyl})_2]\text{ZrCl}_2$ show even greater distortions with tilt angles of ca. 8° .¹⁵ The displacement from planarity at the *ipso* carbon of the cyclopentadienyl rings for the double *ansa*-bridged derivative is not, however, significantly greater than for the single-bridged derivative (Table 1).

Another important aspect in which the structure of $[\text{Me}_2\text{Si}(\text{C}_5\text{H}_4)_2]\text{ZrCl}_2$ differs from that of the double-bridged $[(\text{Me}_2\text{Si})_2(\text{C}_5\text{H}_3)_2]\text{ZrCl}_2$ complex is that the former has a conformation that places an edge of each cyclopentadienyl ring above the central equatorial coordination site of the metallocene fragment (Class IV, Figure 1), whereas the latter has a conformation that

places a vertex of each cyclopentadienyl ring above the central equatorial coordination site (Class III, Figure 1). Furthermore, since the Zr-C bonds involving the bridgehead carbon atoms of $[\text{Me}_2\text{Si}(\text{C}_5\text{H}_4)_2]\text{ZrCl}_2$ and $[(\text{Me}_2\text{Si})_2(\text{C}_5\text{H}_3)_2]\text{ZrCl}_2$ are shorter than the others, the difference in conformation is manifested by a distortion which approaches an " η^2 -ene-allyl" structure for the double *ansa*-bridged complex, rather than the " η^3 -allyl-ene" structure for the single *ansa*-bridged complex.

2. Unbridged Zirconocene Complexes. 2.1. Infrared Spectroscopic Studies. Since the ν_{CO} stretching frequency of a metal carbonyl complex provides a simple means of assessing the electron density on the metal center,^{39,40} we have measured the ν_{CO} stretching frequencies for a series of $(\text{Cp}^{\text{R}})_2\text{Zr}(\text{CO})_2$ derivatives⁴¹ in hydrocarbon solvents, as summarized in Table 2. A plot of $\nu_{\text{CO}(\text{asym})}$ versus $\nu_{\text{CO}(\text{sym})}$ (Figure 4) indicates that cyclopentadienyl substituents do not influence $\nu_{\text{CO}(\text{sym})}$ and $\nu_{\text{CO}(\text{asym})}$ to the same degree, with $\nu_{\text{CO}(\text{asym})} = 1.2[\nu_{\text{CO}(\text{sym})}] - 480$.⁴² In addition to the variation of $\nu_{\text{CO}(\text{asym})}$ and $\nu_{\text{CO}(\text{sym})}$, the relative intensities of these absorptions vary as a function of substituent. For other systems, the $I_{\text{asym}}/I_{\text{sym}}$ ratio has provided a means of determining the $(\text{OC})\text{-M-(CO)}$ bond angle in solution via the expression $\theta = 2 \tan^{-1}\{(I_{\text{asym}}/I_{\text{sym}})\}^{0.5}$.^{42,43} However, for the zirconocene complexes reported here, the angles calculated from the intensity measurements (which fall in the range $103\text{--}109^\circ$) are consistently greater than the values that have been determined by X-ray diffraction on several $(\text{Cp}^{\text{R}})_2\text{Zr}(\text{CO})_2$ derivatives ($83^\circ\text{--}91^\circ$). Thus, we conclude that

(34) Thiele, K. H.; Schliessburg, C.; Baumeister, K.; Hassler, K. *Z. Anorg. Allg. Chem.* **1996**, *622*, 1806–1810.

(35) Zachmanoglou, C. E.; Parkin, G. Unpublished results.

(36) Sitzmann, H.; Zhou, P.; Wolmershauer, G. *Chem. Ber.* **1994**, *127*, 3–9.

(37) O'Hare, D.; Murphy, V.; Diamond, G. M.; Arnold, P.; Mountford, P. *Organometallics* **1994**, *13*, 4689–4694.

(38) Cano, A.; Cuenca, T.; Gomez-Sal, P.; Royo, B.; Royo, P. *Organometallics* **1994**, *13*, 1688–1694.

(39) (a) Collman, J. P.; Hegedus, L. S.; Norton, J. R.; Finke, R. G. *Principles and Applications of Organotransition Metal Chemistry*; University Science Books: Mill Valley, California, 1987. (b) Elschenbroich, C.; Salzer, A. *Organometallics*, 2nd ed.; VCH: New York, 1992. (c) Mingos, D. M. P. in *Comprehensive Organometallic Chemistry*; Wilkinson, G.; Stone, F. G. A., Abel, E. W., Eds.; Pergamon Press: Oxford, U. K., 1982; Vol. 3, Section 19.2.

(40) (a) DeKock, R. L.; Sarapu, A. C.; Fenske, R. F. *Inorg. Chem.* **1971**, *10*, 38–43. (b) Hall, M. B.; Fenske, R. F.; *Inorg. Chem.* **1972**, *11*, 1619–1624. (c) Goldman, A. S.; Krogh-Jespersen, K. *J. Am. Chem. Soc.* **1996**, *118*, 12159–12166. (d) Lupinetti, A. J.; Fau, S.; Frenking, G.; Strauss, S. H. *J. Phys. Chem.* **1997**, *101*, 9551–9559. (e) Lupinetti, A. J.; Frenking, G.; Strauss, S. H. *Angew. Chem., Int. Ed.* **1998**, *37*, 2113–2116. (f) Lupinetti, A. J.; Strauss, S. H.; Frenking, G. *Prog. Inorg. Chem.* **2001**, *49*, 1–112.

(41) For a review of $(\text{Cp}^{\text{R}})_2\text{M}(\text{CO})_2$ ($\text{M} = \text{Ti}, \text{Zr}, \text{Hf}$), see: Sikora, D. J.; Macomber, D. W.; Rausch, M. D. *Carbonyl Derivatives of Titanium, Zirconium, and Hafnium. Adv. Organomet. Chem.* **1986**, *25*, 317–379.

(42) $\nu_{\text{CO}(\text{sym})}$ is greater than $\nu_{\text{CO}(\text{asym})}$ due to the fact that when one C–O bond is stretched it becomes more difficult to stretch the other. The physical basis for this observation is that stretching a C–O bond lowers the energy of the π^* orbital such that it accepts more electron density from the metal center. As a result of stretching one C–O bond, the metal center becomes more electron-deficient and thereby strengthens the C–O bond of the other ligand. Thus, stretching two C–O bonds simultaneously in a symmetric manner is a higher-energy process than the asymmetric version. See: Cotton, F. A.; Wilkinson, G. *Advanced Inorganic Chemistry*, 5th ed.; Wiley-Interscience: New York, 1988; pp 1034–1040.

(43) Kettle, S. F. A.; Paul, I. *Adv. Organomet. Chem.* **1972**, *10*, 199–236.

Table 2. Spectroscopic and Electrochemical Data for (Cp^R)₂Zr(CO)₂ and (Cp^R)₂ZrCl₂

	(Cp ^R) ₂ Zr(CO) ₂				(Cp ^R) ₂ ZrCl ₂		ref to Cp ^R ligands and/or {(Cp ^R) ₂ Zr} derivatives
	$\nu(\text{CO})_{\text{sym}}/\text{cm}^{-1}$ (pentane)	$\nu(\text{CO})_{\text{asym}}/\text{cm}^{-1}$ (pentane)	$\nu(\text{CO})_{\text{av}}/\text{cm}^{-1}$ (pentane)	$\delta(^{13}\text{C})/\text{ppm}$	$E_{\text{red}}^{\circ}/\text{mV}$ (−41 °C, THF)	$\lambda_{\text{max}}/\text{nm}$ ($\epsilon/\text{M}^{-1}\text{cm}^{-1}$) (toluene)	
Methyl Substitution							
Cp ₂ Zr	1976	1888	1932.0	265.4	0	334 (670)	1
(Cp ^{Me₂}) ₂ Zr	1971	1882	1926.5		−51	336 (690)	2
(Cp ^{1,2-Me₂}) ₂ Zr	1966	1877	1921.5		−105	352 (700)	3
(Cp ^{1,2,4-Me₃}) ₂ Zr	1958	1867	1912.5		−150	364 (890)	4
(Cp ^{Me₄}) ₂ Zr	1951	1858	1904.5	274.2 (lit)	−221	362 (900)	5
Cp [*] ₂ Zr	1946	1853	1899.5	273.5	−244	374 (970)	6
Cp(Cp ^{Me₂})Zr	1974	1885	1929.5		−26	334 (860)	
Cp(Cp ^{Me₃})Zr	1964	1874	1919.0		−105	348 (900)	7
Cp(Cp [*])Zr	1965 (lit)	1875 (lit)	1920.0 (lit)		−119	354 (950)	8
(Cp ^{Me})(Cp [*])Zr	1958	1867	1912.5		−154	364 (960)	
Ethyl Substitution							
(Cp ^{Et}) ₂ Zr	1970	1881	1925.5		−56	338 (720)	9
Cp(Cp ^{Et})Zr	1973	1885	1929.0		−26	334 (700)	
Isopropyl Substitution							
(Cp ^{Pr^t}) ₂ Zr	1970	1880	1925.0		−59	348 (690)	10
(Cp ^{1,3-Pr^t₂}) ₂ Zr	1961	1870	1915.5	269.9	−95	356 (740)	
tert-Butyl Substitution							
(Cp ^{Bu^t}) ₂ Zr	1969	1881	1925.0	266.2	−14	346 (760)	11
(Cp ^{1,2-Bu^t₂}) ₂ Zr	1957	1866	1911.5			358 (820)	12
(Cp ^{1,3-Bu^t₂}) ₂ Zr	1958	1868	1913.0		−34	378 (830)	13
Cp(Cp ^{Bu^t})Zr	1972	1884	1928.0				14
Cp(Cp ^{1,3-Bu^t₂})Zr	1968	1879	1923.5			350 (800)	15
Trimethylsilyl Substitution							
(Cp ^{TMS}) ₂ Zr	1972	1886	1929.0		84	346 (700)	16
(Cp ^{1,3-TMS₂}) ₂ Zr	1967	1881	1924.0	264.4 (lit)	61	356 (810)	16
(Cp ^{1,2,4-TMS₃}) ₂ Zr	1964	1881	1922.5	261.3	89	362 (880)	17
Cp(Cp ^{TMS})Zr	1974	1887	1930.5		52	340 (910)	
Cp(Cp ^{1,3-TMS₂})Zr	1973	1888	1930.5		104	346 (910)	
Cp(Cp ^{1,2,4-TMS₃})Zr	1971	1885	1928.0		121	356 (840)	
(Cp ^{TMS})(Cp ^{1,3-TMS₂})Zr	1971	1885	1928.0		79	348 (850)	18
(Cp ^{1,3-TMS})(Cp ^{1,2,4-TMS₃})Zr	1969	1883	1926.0		50	354 (860)	
(Cp ^{TMS₂})(Cp ^{1,2,4-TMS₃})Zr	1967	1880	1923.5				
Other Alkyl Substitution							
Cp [*] (Cp ^{Me₄Et})Zr					−276 (rt)		
(Cp ^{Me₄Et}) ₂ Zr	1946	1854	1900.0	273.1 (lit)	−253		19
Cp [*] (Cp ^{Bu^t})Zr					−166 (rt)		
Cp [*] (Cp ^{1,3-Bu^t₂})Zr					−150 (rt)		
(Cp ^{Bu^t-3,4-Me₂}) ₂ Zr	1955	1863	1909.0		−110	368 (900)	20
Cp[Cp(C ^{Me₂Ph})]Zr	1973	1886	1929.5			344 (960)	
(Cp ^{Me₄TMS}) ₂ Zr	1947	1859	1903.0		−36	380 (1900)	21
(Cp ^{Me₄})(Cp ^{Me₄TMS})Zr	1950	1859	1904.5		−200	362 (1930)	
Cp [*] (Cp ^{Me₄TMS})Zr	1946	1857	1901.5		−145		
Cp [*] (Cp ^{Me₄(CH₂CH₂OMe)})Zr	1937 (lit)	1842 (lit)	1889.5 (lit)				22
(Ind) ₂ Zr	1985 (lit)	1899 (lit)	1942.0 (lit)		110		23
Carbon <i>ansa</i> Bridges							
[H ₂ C(C ₅ H ₄) ₂]Zr					65	366 (900)	24
[(CH ₂ CH ₂)(C ₅ H ₄) ₂]Zr	1976	1886	1931.0		−25	342 (1200)	
[(CH ₂ CH ₂ CH ₂)(C ₅ H ₄) ₂]Zr	1972	1885	1928.5		−68	346 (1280)	25
[Me ₂ C(C ₅ H ₄) ₂]Zr	1978	1892	1935.0		78	348 (1480)	26
<i>rac</i> -[Me ₂ C(C ₅ H ₃ -3-Bu ^t) ₂]Zr	1967	1878	1922.5		14	392 (1580)	27
Silicon <i>ansa</i> Bridges							
[Me ₂ Si(C ₅ H ₄) ₂]Zr	1981	1898	1939.5		118	350 (1000)	28
[Et ₂ Si(C ₅ H ₄) ₂]Zr					116		28
[Pr ₂ Si(C ₅ H ₄) ₂]Zr					115		28
[Me ₂ Si(C ₅ H ₂ -3,4-Me ₂) ₂]Zr	1967	1883	1925.0		−28	372 (1200)	
[Me ₂ Si(C ₅ Me ₄) ₂]Zr	1956	1869	1912.5	271.4	−107	376 (1230)	29
<i>meso</i> -[Me ₂ Si(C ₅ H ₃ -3-Bu ^t) ₂]Zr	1969	1881	1925.0		40	368 (1210)	30
<i>rac</i> -[Me ₂ Si(C ₅ H ₂ -2,4-Bu ^t) ₂]Zr	1962	1878	1920.0	269.1	142	398 (1240)	
<i>rac</i> -[Me ₂ Si(C ₅ H ₂ -2-TMS-4-Bu ^t) ₂]Zr	1967	1888	1927.5		264	404 (1240)	31
<i>rac</i> -[Me ₂ Si(C ₅ H ₂ -2,4-TMS ₂) ₂]Zr					57 (lit)		32
[(Me ₂ SiMe ₂ Si)(C ₅ Me ₄) ₂]Zr	1950	1858	1904.0	274.7	−205	366 (1430)	
Phosphorus <i>ansa</i> Bridges							
[PhP(C ₅ Me ₄) ₂]Zr	1959	1874	1916.5		−4		33
[PhP(O)(C ₅ Me ₄) ₂]Zr					170		33
[PhP(S)(C ₅ Me ₄) ₂]Zr					199		33
[PhP(Se)(C ₅ Me ₄) ₂]Zr					224		33

Table 2 (Continued)

	(Cp ^R) ₂ Zr(CO) ₂				(Cp ^R) ₂ ZrCl ₂		ref to Cp ^R ligands and/or {(Cp ^R) ₂ Zr} derivatives
	$\nu(\text{CO})_{\text{sym}}/\text{cm}^{-1}$ (pentane)	$\nu(\text{CO})_{\text{asym}}/\text{cm}^{-1}$ (pentane)	$\nu(\text{CO})_{\text{av}}/\text{cm}^{-1}$ (pentane)	$\delta(^{13}\text{C})/\text{ppm}$	$E_{\text{red}}^{\circ}/\text{mV}$ (-41 °C, THF)	$\lambda_{\text{max}}/\text{nm}$ ($\epsilon/\text{M}^{-1}\text{cm}^{-1}$) (toluene)	
<i>ansa</i> -Bridged Indenyl							
<i>rac</i> -[(CH ₂ CH ₂ (ind) ₂) ₂ Zr					91	390 (1800)	34
<i>rac</i> -[(CH ₂ CH ₂ (H ₄ ind) ₂) ₂ Zr	1962	1870	1916.0		-100	364 (1880)	34
[(CH ₂ CH ₂ (flu) ₂) ₂ Zr					88	516 (1730)	35
<i>rac</i> -[Me ₂ Si(2-Me-ind) ₂]Zr					102	448 (1940)	36
<i>rac</i> -[Me ₂ Si(2-Me-4-Ph-ind) ₂]Zr					140	464 (1950)	36
Double <i>ansa</i> -Bridges							
[1,1',2,2'-(Me ₂ Si) ₂ (C ₅ H ₃) ₂]Zr					-47	364 (1950)	37
[1,1',2,2'-(Me ₂ Si) ₂ (C ₅ H-3,5-Pr ⁱ)- (C ₅ H ₂ -4-Pr ⁱ)]Zr					-169 (rt)		38,39
[1,1',2,2'-(Me ₂ Si) ₂ (C ₅ H-3,5-Pr ⁱ)- (C ₅ H ₂ -4-TMS)Zr]					-173 (rt)		39
[1,1',2,2'-(Me ₂ Si) ₂ (C ₅ H ₂ -4-Bu ^t) ₂]Zr	1962	1867	1914.5				40
[(1,1'-Me ₂ Si)(2,2'-Me ₂ C)- (C ₅ H ₂ -4-Bu ^t) ₂]Zr	1962	1869	1915.5				41

(1) (a) Fachinetti, G.; Fochi, G.; Floriani, C. *J. Chem. Soc., Chem. Commun.* **1976**, 230–231. (b) Atwood, J. L.; Rogers, R. D.; Hunter, W. E.; Floriani, C.; Fachinetti, G.; Chieslville, A. *Inorg. Chem.* **1980**, *19*, 3812–3817. (2) Jordan, R. F.; Lapointe, R. E.; Bradley, P. K.; Baenziger, N. *Organometallics* **1989**, *8*, 2892–2903. (3) (a) Mengele, W.; Diebold, J.; Troll, C.; Roll, W.; Brintzinger, H. H. *Organometallics* **1993**, *12*, 1931–1935. (b) Harada, M.; Mise, T.; Miya, S.; Yamazaki, H. Eur. Pat. Appl. EP0283739, 1988. (4) Kimura, K.; Takaiishi, K.; Matsukawa, T.; Yoshimura, T.; Yamazaki, H. *Chem. Lett.* **1998**, 571–572. (5) Courtot, P.; Pichon, R.; Salaun, J. Y.; Toupet, L. *Can. J. Chem.* **1991**, *69*, 661–672. (6) Manriquez, J. M.; Bercaw, J. E. *J. Am. Chem. Soc.* **1974**, *96*, 6229–6230. (7) Janiak, C.; Versleeg, U.; Lange, K. C. H.; Weimann, R.; Hahn, E. J. *Organomet. Chem.* **1995**, *501*, 219–234. (8) Wolczanski, P. T.; Bercaw, J. E. *Organometallics* **1982**, *1*, 793–799. (9) Lappert, M. F.; Pickett, C. J.; Riley, P. I.; Yarrow, P. I. W. *J. Chem. Soc., Dalton Trans.* **1981**, 805–813. (10) Kruger, C.; Nolte, M.; Erker, G.; Thiele, S. Z. *Naturforsch. (B)* **1992**, *47*, 995–999. (11) Howie, R. A.; McQuillan, G. P.; Thompson, D. W.; Lock, G. A. *J. Organomet. Chem.* **1986**, *303*, 213–220. (12) Hughes, R. P.; Kowalski, A. S.; Lompney, J. R.; Rheingold, A. L. *Organometallics* **1994**, *13*, 2691–2695. (13) Böhme, U.; Langhof, H. Z. *Kristallogr.* **1993**, *206*, 281–283. (14) Renaut, P.; Tainturier, G.; Gautheron, B. *J. Organomet. Chem.* **1978**, *148*, 35–42. (15) Janiak, C.; Lange, K. C. H.; Versteeg, U.; Lentz, D.; Budzelaar, P. H. M. *Chem. Ber./Recl.* **1996**, *129*, 1517–1529. (16) Antifoliolo, A.; Lappert, M. F.; Singh, A.; Winterborn, D. J. W.; Engelhardt, L. M.; Raston, C. L.; White, A. H.; Carty, A. J.; Taylor, N. J. *J. Chem. Soc., Dalton Trans.* **1987**, 1463–1472. (17) Winter, C. H.; Dobbs, D. A.; Zhou, X.-X. *J. Organomet. Chem.* **1991**, *403*, 145–151. (18) Thiele, K. H.; Bohme, U.; Peters, K.; Peters, E. M.; Walz, L.; Voncherner, H. G. Z. *Anorg. Allg. Chem.* **1993**, *619*, 771–774. (19) (a) Howard, W. A.; Waters, M.; Parkin, G. *J. Am. Chem. Soc.* **1993**, *115*, 4917–4918. (b) Howard, W. A.; Trnka, T. M.; Waters, M.; Parkin, G. *J. Organomet. Chem.* **1997**, *528*, 95–121. (20) Sauvageot, P.; Moise, C. *Bull. Soc. Chim. Fr.* **1996**, *133*, 177–182. (21) Horacek, M.; Gypes, R.; Cisarova, I.; Polasek, M. *Collect. Czech. Chem. Commun.* **1996**, *61*, 1307–1320. (22) (a) Krut'ko, D. P.; Borzov, M. V.; Petrosyan, V. S.; Kuz'mina, L. G.; Churakov, A. V. *Russ. Chem. Bull.* **1996**, *45*, 1740–1744. (b) Krut'ko, D. P.; Borzov, M. V.; Kuz'mina, L. G.; Churakov, A. V.; Lemenovskii, D. A.; Reutov, O. A. *Inorg. Chim. Acta* **1998**, *280*, 257–263 (IR data). (23) Samuel, E.; Setton, R. *J. Organomet. Chem.* **1965**, *4*, 156–158. (24) Katz, T. J.; Acton, N. *Tetrahedron Lett.* **1970**, 2497–2499. (25) Hillman, M.; Weiss, A. *J. Organomet. Chem.* **1972**, *42*, 123–128. (26) (a) Nifant'ev, I. E.; Butakov, K. A.; Aliev, Z. G.; Urazovskii, I. F. *Metallorg. Khim.* **1991**, *4*, 1265–1268. (b) Quijada, R.; DuPont, J.; Correa Silveira, D.; Lacerda Miranda, M. S.; Scipioni, R. B. *Macromol. Rapid Commun.* **1995**, *16*, 357–362. (27) Urazowski, I. F.; Atovmyan, L. O.; Mkoyan, S. G.; Broussier, R.; Perron, P.; Gautheron, B.; Robert, F. *J. Organomet. Chem.* **1997**, *536*–537, 531–536. (28) Bajgur, C. S.; Tikkanen, W. R.; Petersen, J. L. *Inorg. Chem.* **1985**, *24*, 2539–2546. (29) Jutzi, P.; Dickbreder, R. *Chem. Ber.* **1986**, *119*, 1750–1754. (30) Wiesenfeldt, H.; Reinmuth, A.; Barsties, E.; Evertz, K.; Brintzinger, H. H. *J. Organomet. Chem.* **1989**, *369*, 359–370. (31) Chacon, S. T.; Coughlin, E. B.; Henling, L. M.; Bercaw, J. E. *J. Organomet. Chem.* **1995**, *497*, 171–180. (32) Langmaker, J.; Samec, Z.; Varga, V.; Horacek, M.; Choukroun, R.; Mach, K. *J. Organomet. Chem.* **1999**, *584*, 323–328. (33) Shin, J. H.; Hascall, T.; Parkin, G. *Organometallics* **1999**, *18*, 6–9. (34) Kaminsky, W.; Kulper, K.; Brintzinger, H. H.; Wild, F. R. W. P. *Angew. Chem., Int. Ed. Engl.* **1985**, *24*, 507–508. (35) (a) Chen, Y.-X.; Rausch, M. D.; Chien, J. C. W. *Macromolecules* **1995**, *28*, 5399–5404. (b) Alt, H. G.; Milius, W.; Palackal, S. J. *J. Organomet. Chem.* **1994**, *472*, 113–118. (36) Spaleck, W.; Antberg, M.; Rohrmann, J.; Winter, A.; Bachmann, B.; Kiprof, P.; Behm, J.; Hermann, W. A. *Angew. Chem., Int. Ed. Engl.* **1992**, *31*, 1347–1350. (37) Cano, A.; Cuenca, T.; Gomezsal, P.; Royo, P. *Organometallics* **1994**, *13*, 1688–1694. (38) Veghini, D.; Day, M. W.; Bercaw, J. E. *Inorg. Chim. Acta* **1998**, *280*, 226–232. (39) Bercaw, J. E.; Herzog, T. A. U.S. Patent 5,708,101, 1998. (40) (a) Chirik, P. J.; Henling, L. M.; Bercaw, J. E. *Organometallics* **2001**, *20*, 534–544. (b) Bulls, A. R. Ph.D. Thesis, California Institute of Technology, 1998. (41) Brandow, C. G.; Bercaw, J. E. Unpublished results.

the intensity measurements are not sufficiently reliable in this system to allow accurate determination of (OC)–Zr–(CO) bond angle.⁴⁴

Due to the different sensitivities of $\nu_{\text{CO}(\text{asym})}$ and $\nu_{\text{CO}(\text{sym})}$ to a ring substituent, the average value, $\nu_{\text{CO}(\text{av})}$, is used for comparison purposes to describe the electronic influence of cyclopentadienyl ring substituents in the following discussion. The effect of a simple methyl substituent provides a textbook example of the trend one would expect, with increasing substitution causing a reduction of $\nu_{\text{CO}(\text{av})}$ (Table 2 and Figure 5). Consideration of the (Cp^{Me_n})₂Zr(CO)₂ series, and also mixed ring derivatives such as CpCp*Zr(CO)₂, indicates that each methyl substituent on average reduces $\nu_{\text{CO}(\text{av})}$ by 3.2 cm⁻¹. Superimposed on this figure are the available data for ethyl,

isopropyl, *tert*-butyl, and trimethylsilyl derivatives, which clearly indicate that the *tert*-butyl substituent has the greatest effect. Consideration of the additional data in Table 3 indicates that the overall electron-donating influence of a substituent, as judged by $\nu_{\text{CO}(\text{av})}$, follows the sequence Bu^t > Prⁱ ≈ Et ≈ Me > Me₃Si > H, a trend which follows their inductive power as judged by Hammett σ_{meta} values (vide infra). Significantly, the data also indicate that the influence of substituents on $\nu_{\text{CO}(\text{av})}$ is not particularly sensitive to their location. For example $\nu_{\text{CO}(\text{av})}$ for (Cp^{1,2-Bu^t})₂Zr(CO)₂ (1912 cm⁻¹) and (Cp^{1,3-Bu^t})₂Zr(CO)₂ (1912 cm⁻¹) are identical; likewise, $\nu_{\text{CO}(\text{av})}$ for complexes in which the substituents are in different rings, for example, Cp(Cp^{Me₄})₂Zr(CO)₂ (1919 cm⁻¹) and (Cp^{1,2-Me₂})₂Zr(CO)₂ (1922 cm⁻¹), are also very similar.

2.2. Electrochemical Studies. Zirconocene derivatives (Cp^R)₂ZrX₂ have been the subject of numerous electrochemical studies,^{45,46} with the earliest report dating back to 1966.^{45a,47} These studies indicate that one-electron reduction of (Cp^R)₂Zr-

(44) Although not sufficiently accurate to allow determination of the (OC)–Zr–(CO) bond angle in zirconocene complexes, IR intensity measurements are able to distinguish *cis* versus *trans* geometries of dicarbonyl compounds. See, for example: Cotton, F. A.; Lukehart, C. M. *J. Am. Chem. Soc.* **1971**, *93*, 2672–2676.

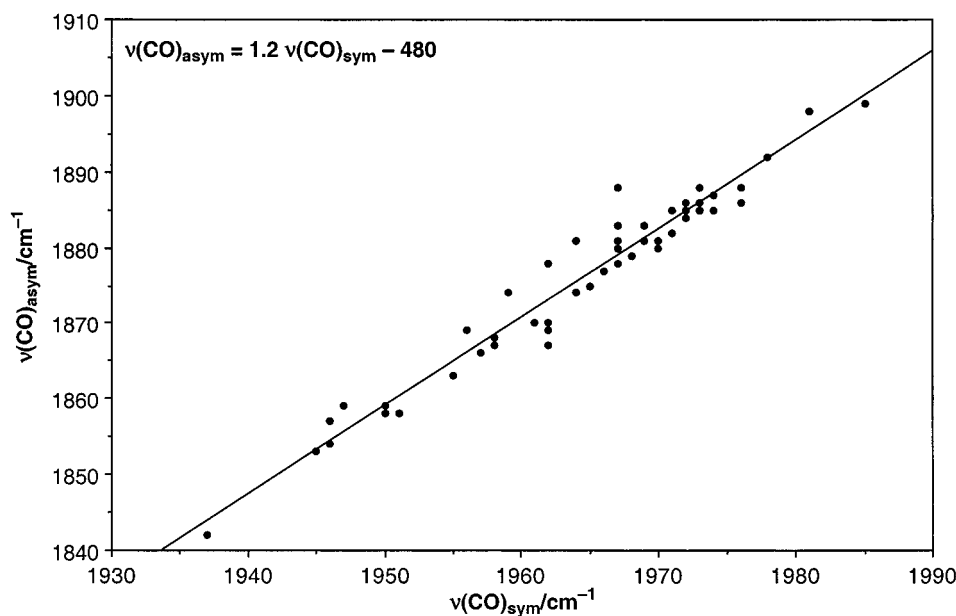


Figure 4. Correlation of $\nu_{\text{CO(asy)}}$ and $\nu_{\text{CO(sym)}}$ for $(\text{Cp}^{\text{R}})_2\text{Zr}(\text{CO})_2$ derivatives.

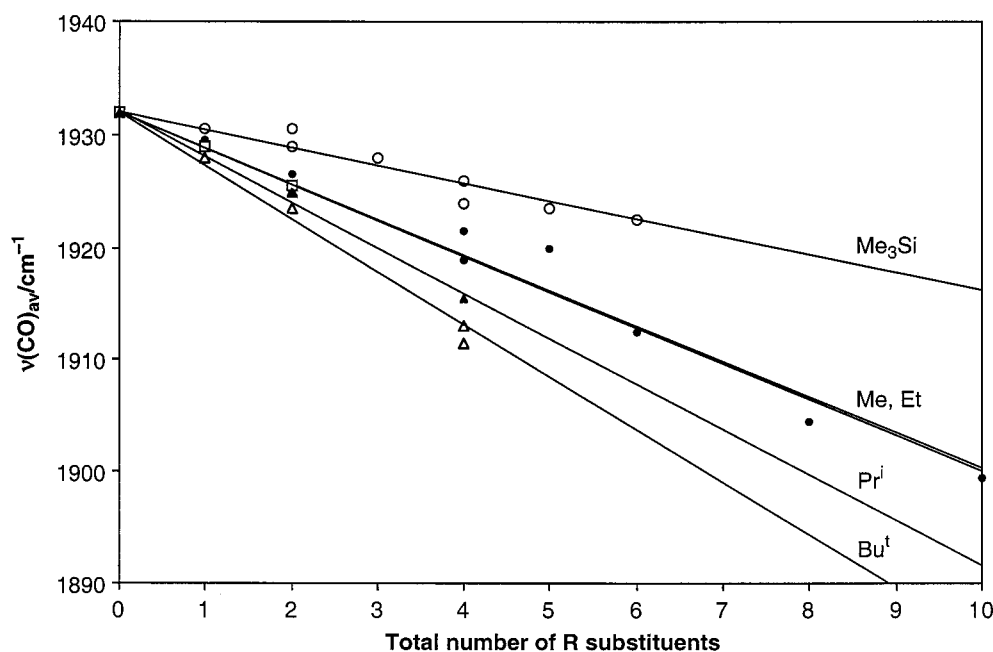


Figure 5. Influence of substituents on $\nu_{\text{CO(av)}}$ of $(\text{Cp}^{\text{R}})_2\text{Zr}(\text{CO})_2$.

ZrX_2 giving $[(\text{Cp}^{\text{R}})_2\text{ZrX}_2]^-$ is often reversible and that the reduction potentials yield information pertaining to the electron-donating capability of the ring substituents. However, the

accuracy of the reduction potential measurements casts doubt over certain interpretations. Consider, for example, the literature pertaining to the influence of a Me_3Si group on the redox properties of $(\text{Cp}^{\text{R}})_2\text{ZrX}_2$. In 1981, Lappert reported that the reduction potential of Cp_2ZrCl_2 (-1.70 V) is more negative than that of $(\text{Cp}^{\text{TMS}})_2\text{ZrCl}_2$ (-1.59 V),⁴⁸ thereby indicating that the

(45) See, for example: (a) Dessy, R. E.; King, R. B.; Waldrop, M. A. *J. Am. Chem. Soc.* **1966**, *88*, 5112–5117. (b) Samuel, E.; Guery, D.; Vedel, J.; Basile, F. *Organometallics* **1985**, *4*, 1073–1077. (c) Lappert, M. F.; Pickett, C. J.; Riley, P. I.; Yarrow, P. I. W. *J. Chem. Soc., Dalton Trans.* **1981**, 805–813. (d) Bajgur, C. S.; Tikkanen, W. R.; Petersen, J. L. *Inorg. Chem.* **1985**, *24*, 2539–2546. (e) Langmaier, J.; Samec, Z.; Varga, V.; Horacek, M.; Choukroun, R.; Mach, K. *J. Organomet. Chem.* **1999**, *584*, 323–328. (f) Loukova, G. V.; Babkina, O. N.; Bazhenova, T. A.; Bravaya, N. M.; Strelets, V. V. *Russ. Chem. Bull.* **2000**, *49*, 60–63. (g) Fakh, A.; Mugnier, Y.; Gautheron, B.; Laviron, E. *J. Organomet. Chem.* **1986**, *302*, C7–C9. (h) Lappert, M. F.; Raston, C. L. *J. Chem. Soc., Chem. Commun.* **1980**, 1284–1285. (i) Lappert, M. F.; Raston, C. L.; Skelton, B. W.; White, A. H. *J. Chem. Soc., Dalton Trans.* **1997**, 2895–2902. (j) Babkina, O. N.; Bazhenova, T. A.; Bravaya, N. M.; Strelets, V. V.; Antipin, M. Yu.; Lysenko, K. A. *Russ. Chem. Bull.* **1996**, *45*, 1458–1465.

(46) Loukova, G. V.; Strelets, V. V. *Collect. Czech. Chem. Commun.* **2001**, *66*, 185–206.

(47) For related electrochemical studies on titanocene derivatives, see: (a) Langmaier, J.; Samec, Z.; Varga, V.; Horacek, M.; Mach, K. *J. Organomet. Chem.* **1999**, *579*, 348–355. (b) Mugnier, Y.; Fakh, A.; Fauconet, M.; Moise, C.; Laviron, E. *Acta Chem. Scand.* **1983**, *B 37*, 423–427. (c) Schwemlein, H.; Tritschler, W.; Kiesele, H.; Brintzinger, H. H. *J. Organomet. Chem.* **1985**, *293*, 353–364. (d) Mugnier, Y.; Moise, C.; Laviron, E. *J. Organomet. Chem.* **1981**, *204*, 61–66. (e) Fussing, I. M. M.; Pletcher, D.; Whitby, R. J. *J. Organomet. Chem.* **1994**, *470*, 119–125. (f) El Murr, N.; Chaloyard, A. *J. Organomet. Chem.* **1981**, *212*, C39–C42. (g) El Murr, N.; Chaloyard, A.; Tirouflet, J. *J. Chem. Soc., Chem. Commun.* **1980**, 446–448. (h) Kotz, J. C.; Vining, W.; Coco, W.; Rosen, R.; Dias, A. R.; Garcia, M. H., *Organometallics* **1983**, *2*, 68–79.

(48) These values are relative to the saturated calomel electrode.

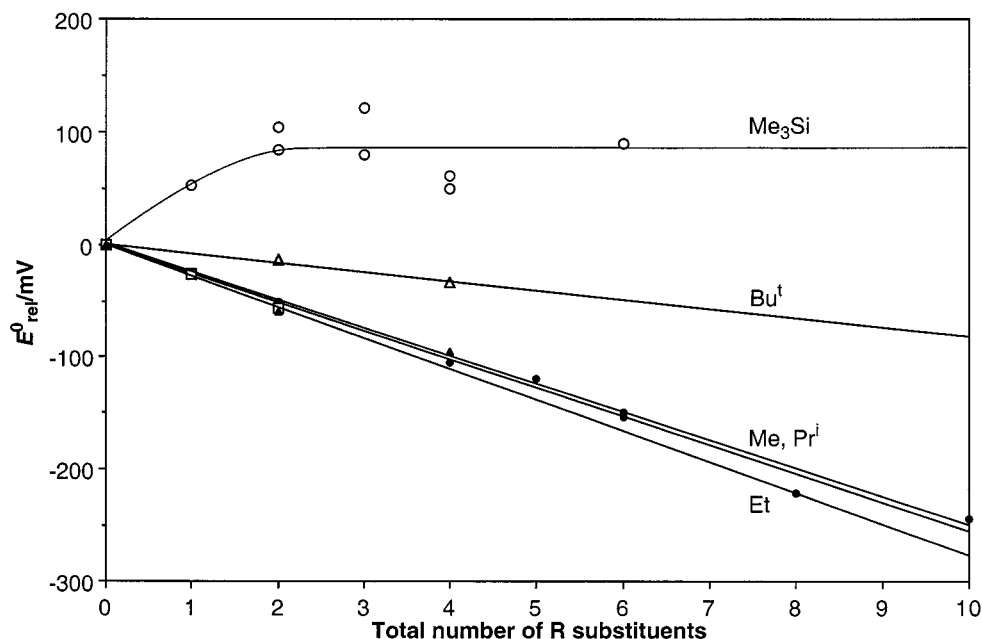


Figure 6. Influence of substituents on E° of $(\text{Cp}^{\text{R}})_2\text{ZrCl}_2$.

Table 3. Substituent Effects on $\nu_{\text{CO}(\text{av})}$ and E°

	σ_{meta}^a	$\Delta\nu$ per subst (cm^{-1})	ΔE° per subst (mV)
H	0	0	0
Me_3Si	-0.04	-1.6	+21.1 to $\sim 0^b$
Me	-0.07	-3.2	-25.5
Et	-0.07	-3.2	-27.6
Pr^i	-0.07	-4.1	-25.1
Bu^t	-0.10	-4.7	-8.2

^a Reference 54d. ^b The value of 21.1 for ΔE° is that of the least-squares fit constrained to go through the value for Cp_2ZrCl_2 ; the unconstrained value is ~ 0 .

Me_3Si group has a poor electron-donating ability relative to that of H.^{45d} These values were revised by Lappert in 1989 [Cp_2ZrCl_2 (-1.60 V) and $(\text{Cp}^{\text{TM}_5})_2\text{ZrCl}_2$ (-1.56 V)],⁴⁹ indicating that the difference is not as great as previously suggested. More recently, Langmaier has studied the electrochemistry of zirconocene complexes with more than one Me_3Si group and has concluded that this substituent has a negligible effect on the reduction potential,^{45e} reporting that the reduction potentials of $[\text{C}_5\text{H}_4(\text{SiMe}_3)_2\text{ZrCl}_2]$, $[\text{C}_5\text{H}_3(\text{SiMe}_3)_2\text{ZrCl}_2]$, and $[\text{C}_5\text{H}_2(\text{SiMe}_3)_3\text{ZrCl}_2]$ are identical. Langmaier also noted that these results are in contrast to those of Choukroun and Dahan who reported that $[\text{C}_5\text{H}_2(\text{SiMe}_3)_3\text{ZrCl}_2]$ does not yield reduction or oxidation waves in the range -3.0 to +1.0 V.⁵⁰ In view of such contradictory reports, we consider it essential to determine accurately the relative reduction potentials to be able to use this technique for probing electronic changes at the zirconium center in $(\text{Cp}^{\text{R}})_2\text{ZrCl}_2$ derivatives. Another problem with the reliability of the reduction potential data for $(\text{Cp}^{\text{R}})_2\text{ZrCl}_2$ is concerned with their electrochemical reversibility, with previous studies having indicated that increasing substitution of the cyclopentadienyl rings reduces the reversibility.^{45e} Therefore, to obtain more meaningful comparative data, we have determined the reduction potentials of a large series of $(\text{Cp}^{\text{R}})_2\text{ZrCl}_2$ derivatives at low

temperature and in a common solvent medium, that is, THF at -41°C with $[\text{Bu}^n_4\text{N}][\text{PF}_6]$ as supporting electrolyte. Furthermore, due to the confusion that often exists with ambiguous referencing protocols,⁵¹ we have elected to report the reduction potentials of $(\text{Cp}^{\text{R}})_2\text{ZrCl}_2$ relative to that of Cp_2ZrCl_2 (Table 2),⁵² which also facilitates a more direct indication of a substituent effect.

Examination of the data in Table 2 and Figure 6 indicates that the progressive incorporation of a methyl group results in a smooth shift of the reduction potentials to more negative values, as illustrated by the $(\text{C}_5\text{Me}_n\text{H}_{5-n})_2\text{ZrCl}_2$ series. Furthermore, a plot of E°_{rel} versus the number of methyl substituents for a series of complexes, which also includes mixed ring derivatives, for example, $\text{CpCp}^*\text{ZrCl}_2$, indicates that a methyl group reduces E° by an average of 25.5 mV. For comparison, a decrease of 36 mV per methyl group was previously reported for the $(\text{C}_5\text{Me}_n\text{H}_{5-n})_2\text{ZrCl}_2$ series, with the exception of $(\text{C}_5\text{Me}_5)_2\text{ZrCl}_2$ for which the reduction potential was anomalous, being more positive than that for $(\text{C}_5\text{HMe}_4)_2\text{ZrCl}_2$.^{45e} Since such a result was counter to that expected on the basis of simple additive inductive effects, Langmaier attributed the exceptional E° value for $(\text{C}_5\text{Me}_5)_2\text{ZrCl}_2$ to steric congestion between the cyclopentadienyl ligands, thereby increasing the $\text{Cp}_{\text{cent}}\text{-Zr-Cp}_{\text{cent}}$ angle and reducing the energy difference between the frontier orbitals.^{45e} However, such an explanation is no longer required since it is evident that the E° value for $(\text{C}_5\text{Me}_5)_2\text{ZrCl}_2$ is not exceptional. Although the available data are not as extensive for the bulkier substituents, comparison of the E° data for the complexes $(\text{Cp}^{\text{R}})_2\text{ZrCl}_2$ ($\text{R} = \text{H}, \text{Me}, \text{Et}, \text{Pr}^i, \text{and Bu}^t$) indicate that all alkyl substituents are electron-donating relative to H: H (0 mV), Me (-25.5 mV per substituent), Et (-27.6 mV per substituent), Pr^i (-25.1 mV per substituent), Bu^t (-8.2 mV per substituent). Interestingly, by comparison to Me, Et, and Pr^i substituents, which exert a comparable electron-donating

(49) Antiñolo, A.; Bristow, G. S.; Campbell, G. K.; Duff, A. W.; Hitchcock, P. B.; Kamarudin, R. A.; Lappert, M. F.; Norton, R. J.; Sarjudeen, N.; Winterborn, D. J. W.; Atwood, J. L.; Hunter, W. E.; Zhang, H. *Polyhedron* **1989**, *8*, 1601-1606.

(50) Choukroun, R.; Dahan, F. *Organometallics* **1994**, *13*, 2097-2100.

(51) See, for example: Pavlishchuk, V. V.; Addison, A. W. *Inorg. Chim. Acta* **2000**, *298*, 97-102.

(52) Under the conditions reported here, E° for $\text{Cp}_2\text{ZrCl}_2/[\text{Cp}_2\text{ZrCl}_2]^-$ is -2.253 V relative to $\text{Cp}_2\text{Fe}^+/\text{Cp}_2\text{Fe}$.

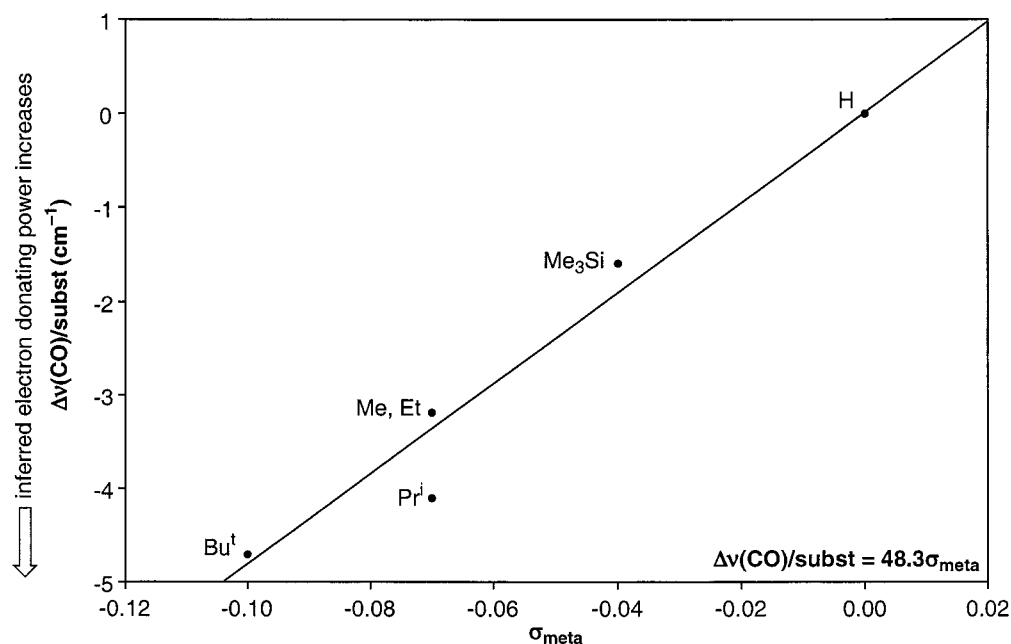


Figure 7. Correlation of the change in $\nu_{\text{CO(av)}}$ per substituent of $(\text{Cp}^{\text{R}})_2\text{Zr}(\text{CO})_2$ with Hammett σ_{meta} values.

effect as judged by the reduction potentials of monosubstituted $(\text{Cp}^{\text{R}})_2\text{ZrCl}_2$, the Bu^{t} substituent exhibits a small effect (Table 3). Comparison of the effect of disubstituted derivatives reinforces this observation. Thus, the reduction potential of $(\text{Cp}^{1,2-\text{Me}_2})_2\text{ZrCl}_2$ (-105 mV) is considerably more negative than that of $(\text{Cp}^{1,3-\text{Bu}^{\text{t}}})_2\text{ZrCl}_2$ (-34 mV).

In contrast to the observation that alkyl substitution causes the reduction potentials for $(\text{Cp}^{\text{R}})_2\text{ZrCl}_2$ to shift to more negative values compared to Cp_2ZrCl_2 , the incorporation of Me_3Si substituents results in a positive shift relative to Cp_2ZrCl_2 , thereby corresponding to an electron-withdrawing effect. For example, the E° values for the trimethylsilyl derivatives listed in Table 2 are 50–121 mV more positive than the value for Cp_2ZrCl_2 ,⁵³ with an average increase of 21.1 mV per substituent. However, the scatter in the plot of E° versus number of Me_3Si groups is significant (Figure 6), and if the value for Cp_2ZrCl_2 is omitted from the least-squares fit, a Me_3Si group is seen to exert only a small effect on E° for the incremental incorporation of Me_3Si groups. Langmaier also noted that a Me_3Si group exerts a negligible effect on E° for a subset of the complexes studied here,^{45c} and thus it is apparent that a leveling effect is observed upon incorporation of Me_3Si groups. The electron-donating ability of a substituent, as judged by its influence on E° , therefore follows the sequence $\text{Me} > \text{Bu}^{\text{t}} > \text{H} \geq \text{Me}_3\text{Si}$.

2.3. Comparison of Trends in ν_{CO} and E° . A most interesting aspect of the IR spectroscopic and electrochemical studies on $(\text{Cp}^{\text{R}})_2\text{Zr}(\text{CO})_2$ and $(\text{Cp}^{\text{R}})_2\text{ZrCl}_2$, respectively, is that the conclusions pertaining to the relative electron-donating properties of the ring substituents are influenced by the method used to probe the effect, as summarized by the $\Delta\nu_{\text{CO}}$ per substituent and ΔE° per substituent values listed in Table 3. Thus, while the electron-donating trend inferred by the variation of ν_{CO} is consistent with simple inductive effects ($\text{Bu}^{\text{t}} > \text{Me} >$

$\text{Me}_3\text{Si} > \text{H}$),⁵⁴ that based on E° is anomalous ($\text{Me} > \text{Bu}^{\text{t}} > \text{H} \geq \text{Me}_3\text{Si}$), as illustrated by comparison of Figures 7 and 8. As such, the correlation between ν_{CO} and E° is poor (Figure 9). For example, whereas consideration of both ν_{CO} and E° values indicates that a methyl group is electron-donating relative to hydrogen, a trimethylsilyl group is electron-donating as judged by ν_{CO} , but inferred to be electron-withdrawing as judged by E° . The situation is further complicated by the fact that X-ray photoelectron spectroscopic analysis of the transition-metal center of zirconocenes, hafnocenes, and ferrocenes having trimethylsilyl substituents on the cyclopentadienyl rings indicate yet another order of inferred electron-donating abilities ($\text{Me}_3\text{Si} > \text{Me} > \text{H}$), as summarized in Table 4.⁵⁵

Dichotomies of this type, with different electron-donating abilities being inferred by different techniques, have been previously reported (Table 4). For example, whereas consideration of the ionization energies of series of alkylnickelocene complexes $(\text{Cp}^{\text{R}})_2\text{Ni}$ imply that the electron-donating properties follow the sequence $\text{Bu}^{\text{t}} > \text{Et} > \text{Me} > \text{H}$, Richardson has noted that consideration of electron affinities suggests that the electron-donating properties follow the sequence $\text{Me} > \text{H} > \text{Et} > \text{Bu}^{\text{t}}$.^{56,57} Moreover, larger alkyl groups exert an electron-withdrawing effect on the electron affinities of ruthenium tris- $(\beta$ -diketonate) derivatives, $\text{Ru}[\eta^2\text{-OC}(\text{R})\text{CHC}(\text{R})\text{O}]_3$, whereas the ionization energies follow the usual electron-donating trend

(54) (a) Hansch, C.; Leo, A.; Taft, R. W. *Chem. Rev.* **1991**, *91*, 165–195. (b) Levitt, L. S.; Widing, H. F. *Prog. Phys. Org. Chem.* **1976**, *12*, 119–157. (c) Taft, R. W.; Topsom, R. D. *Prog. Phys. Org. Chem.* **1987**, *16*, 1–83. (d) Hansch, C.; Leo, A.; Unger, S. H.; Kim, K. H.; Nikaitani, D.; Lien, E. *J. Med. Chem.* **1973**, *16*, 1207–1216.

(55) Specifically, the binding energy of the inner-shell electrons of the complexed transition metal decreases by 0.10 eV/ Me_3Si group. By this criterion, the electron-donating characteristics of Me_3Si is ca.1.25 more electron-donating than that of Me. See ref 17.

(56) Richardson, D. E.; Ryan, M. F.; Khan, M. N. I.; Maxwell, K. A. *J. Am. Chem. Soc.* **1992**, *114*, 10482–10485.

(57) Furthermore, the electron affinities of RO^\bullet radicals increase in the order $\text{Me} < \text{Et} < \text{Pr}^{\text{i}} < \text{Bu}^{\text{t}}$, suggesting that the electron-donating properties follow the reverse order $\text{Me} > \text{Et} > \text{Pr}^{\text{i}} > \text{Bu}^{\text{t}}$. See: (a) Ellison, G. B.; Engelking, P. C.; Lineberger, W. C. *J. Phys. Chem.* **1982**, *86*, 4873–4878. (b) Janousek, B. K.; Brauman, J. in *Gas-Phase Ion Chemistry*; Bowers, M. T., Ed.; Academic Press: New York, 1984; Vol 2.

(53) A similar result is observed for the more heavily substituted system, and $(\text{Cp}^{\text{Me}_2})_2\text{ZrCl}_2$ (-221 mV), $(\text{Cp}^{\text{Me}_2\text{TMS}})_2\text{ZrCl}_2$ (-36 mV), corresponding to an increase of +93 mV per Me_3Si substituent.

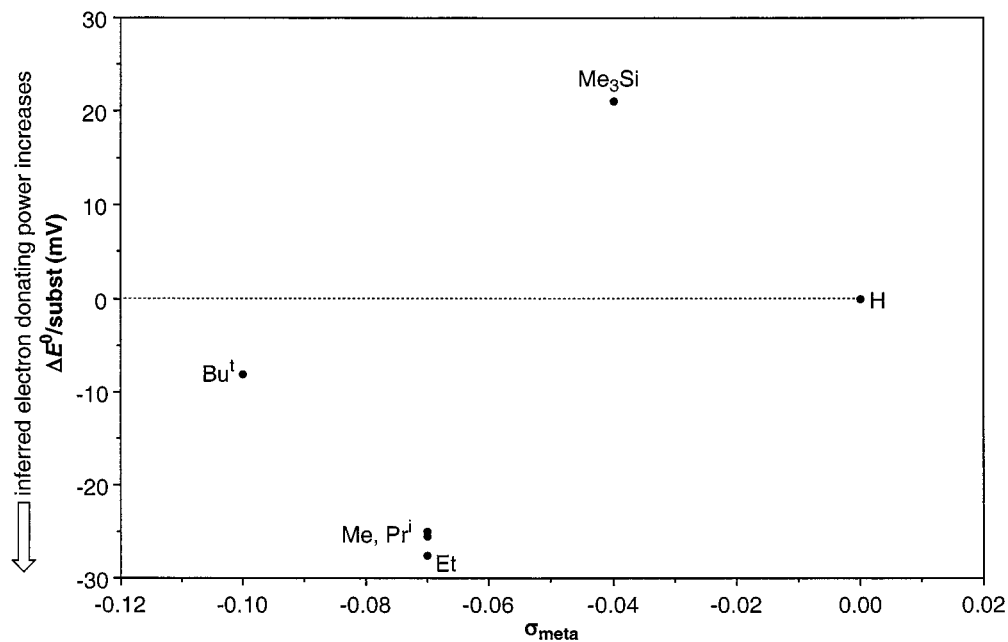


Figure 8. Change in E° per substituent of $(\text{Cp}^{\text{R}_n})_2\text{ZrCl}_2$ with Hammett σ_{meta} values, indicating a lack of correlation.

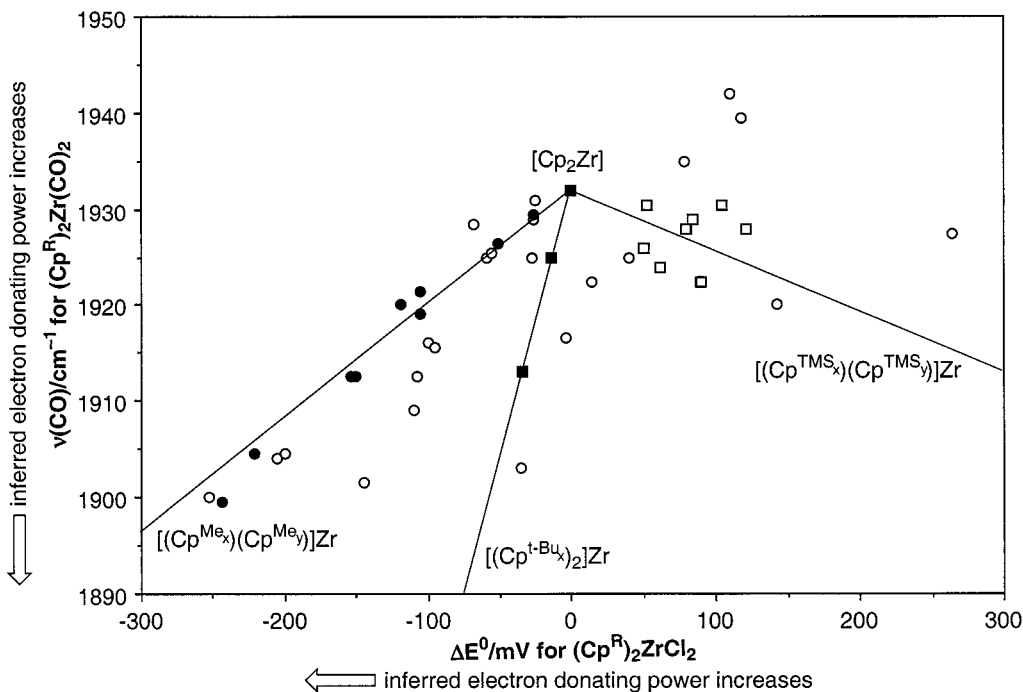


Figure 9. Poor correlation of substituent effects for $\nu_{\text{CO(av)}}$ of $(\text{Cp}^{\text{R}_n})_2\text{Zr}(\text{CO})_2$ and E° of $(\text{Cp}^{\text{R}_n})_2\text{ZrCl}_2$. Lines are drawn for the points corresponding to Me (●), Bu^t (■), and Me_3Si (□) substituted derivatives. Note that trends in both $\nu_{\text{CO(av)}}$ and E° values infer a common electron-donating effect for Me substituents, whereas they are opposed for Me_3Si substituents.

based on Hammett σ_{meta} constants.^{58,59} Richardson has, therefore, commented that alkyl substituent effects cannot be uniformly described as “electron-donating” and has proposed a model based on a combination of inductive and polarization effects.⁵⁶ In this model, the inductive effect stabilizes a positive charge, whereas the polarization effect stabilizes both positive and negative charges remote from the substituent.^{60,61} By analogy

with electron affinities, E° is also influenced by polarization effects that stabilize the anion $[(\text{Cp}^{\text{R}_n})_2\text{ZrCl}_2]^-$. Thus, a Bu^t group exerts less of an “electron-donating” effect than a Me group because the polarization effect of the larger Bu^t group stabilizes the negative charge of the anion $[(\text{Cp}^{\text{R}_n})_2\text{ZrCl}_2]^-$ and thereby reduces its destabilizing inductive effect. For reference, the following polarizability parameters ($\sigma_{\alpha(\text{X})}$) have been

(58) Sharpe, P.; Alameddini, N. G.; Richardson, D. E. *J. Am. Chem. Soc.* **1994**, *116*, 11098–11108.

(59) It should be noted that the solution $\text{Ru}^{\text{III}}/\text{Ru}^{\text{II}}$ potentials exhibit the opposite trend due to solvation obscuring the intrinsic effect of alkyl substituent. See ref 58.

(60) The polarizability effect has a $1/r^4$ dependence, whereas inductive effects have a $1/r^2$ dependence. See ref 54c and Hehre, W. J.; Pau, C.-P.; Headley, A. D.; Taft, R. W.; Topsom, R. D. *J. Am. Chem. Soc.* **1986**, *108*, 1711–1712.

(61) For example, Bu^tO^- in the gas phase is less basic than MeO^- . See: Brauman, K. I.; Blair, L. K. *J. Am. Chem. Soc.* **1968**, *90*, 6561–6562.

Table 4. Inferred Electron-Donating Ability of a Substituent According to Method

technique	inferred electron-donating ability	ref
Hammett σ_{meta} , pK_{a} ($m\text{-XC}_6\text{H}_4\text{CO}_2\text{H}$)	Bu ^t > Pr ⁱ \approx Et \approx Me > Me ₃ Si > H	<i>a</i>
ν_{CO} IR of (Cp ^R) ₂ Zr(CO) ₂	Bu ^t > Me > Me ₃ Si > H	this work
IP of (Cp ^R) ₂ Ni	Bu ^t > Et > Me > H	<i>b</i>
IP of Ru[$\eta^2\text{-OC(R)CHC(R)O}$] ₃	Bu ^t > Pr ⁱ > Et > Me	<i>c</i>
E° of (Cp ^R) ₂ ZrCl ₂	Me > Bu ^t > H \geq Me ₃ Si	this work
EA of (Cp ^R) ₂ Ni	Me > H > Et > Bu ^t	<i>b</i>
EA of Ru[$\eta^2\text{-OC(R)CHC(R)O}$] ₃	Me > Et > Pr ⁱ > Bu ^t	<i>c</i>
EA of RO [*]	Me > Et > Pr ⁿ > H > Pr ⁱ > Bu ^t	<i>d</i>
XPS of (Cp ^R) ₂ MCl ₂	Me ₃ Si > Me > H	<i>e</i>

^a Hansch, C.; Leo, A.; Taft, R. W. *Chem. Rev.* 1991, 91, 165–195. ^b Richardson, D. E.; Ryan, M. F.; Khan, M. N. I.; Maxwell, K. A. *J. Am. Chem. Soc.* 1992, 114, 10482–10485. ^c Sharpe, P.; Alameddini, N. G.; Richardson, D. E. *J. Am. Chem. Soc.* 1994, 116, 11098–11108. ^d Ellison, G. B.; Engelking, P. C.; Lineberger, W. C. *J. Phys. Chem.* 1982, 86, 4873–4878. ^e Gassman, P. G.; Deck, P. A.; Winter, C. H.; Dobbs, D. A.; Cao, D. H. *Organometallics* 1992, 11, 959–960.

derived:⁶² H (0.0), Me (−0.35), Et (−0.49), Prⁱ (−0.54), Bu^t (−0.75), SiMe₃ (−0.72). The relatively large negative values for the Bu^t and SiMe₃ substituents indicate that they are particularly effective at stabilizing negative charge by a polarization mechanism.⁶³ Thus, the positive shift in the reduction potential of (Cp^{TMS})₂ZrCl₂ relative to Cp₂ZrCl₂ is not a consequence of the poor inductive effect of a trimethylsilyl group, as has been previously proposed,^{45d} but is rather more likely a result of significant polarization contribution.⁶⁴ Differential solvation of (Cp^R)₂ZrCl₂ and [(Cp^R)₂ZrCl₂][−] will also provide an additional means of modulating E°_{rel} from the value expected on the basis of substituent inductive effects.

In contrast to E°_{rel} , which is related to the energy difference between neutral and anionic molecules, ν_{CO} is a feature of a single neutral molecule. Polarization and solvation effects are, therefore, unlikely to play a significant role in influencing ν_{CO} . As such, the electron-donating trend inferred by the variation of ν_{CO} with a substituent is dictated by inductive effects. For example, evidence that inductive effects are dominant in influencing ν_{CO} is provided by the good correlation of $\Delta\nu_{\text{CO}}$ per substituent with its Hammett σ_{meta} parameter (Figure 7).⁶⁵ Therefore, we conclude that ν_{CO} stretching frequencies provide the better simple method for determining the electronic impact of a substituent on a zirconium center.

X-ray photoelectron studies on the influence of methyl substitution on unbridged titanocene⁶⁶ and hafnocene⁶⁷ derivatives, coupled with calculations, have also concluded that the impact of the substituent is due to an inductive effect and is not due to structural changes induced by increasing the steric demands of the substituted cyclopentadienyl ligands. Specifically, Ti (2p) binding energy calculations of Cp₂TiCl₂ with rings

located in positions corresponding to other (Cp^R)₂TiCl₂ derivatives demonstrated that the calculated binding energy is not very sensitive to the location of the Cp rings and, therefore, is influenced mainly by the inductive effect of the substituents.⁶⁶ Likewise, ⁹¹Zr NMR spectroscopic studies of zirconocene derivatives indicate that the influence of a substituent on the ⁹¹Zr chemical shift is predominantly due to inductive effects and not due to structural changes.⁶⁸ However, other studies suggest that the ⁹¹Zr NMR spectroscopic shift is sensitive to geometrical changes.^{69,70}

At this point it is pertinent to summarize the various methods that have been used to infer electron-donating abilities. Examination of Table 4 indicates that, of these methods, the ν_{CO} stretching frequencies of (Cp^R)₂Zr(CO)₂ and the ionization potentials of (Cp^R)₂Ni and Ru[$\eta^2\text{-OC(R)CHC(R)O}$]₃ all exhibit trends that are in line with the conventional order of electron-donating abilities as suggested by Hammett σ_{meta} values. However, techniques that involve reduction (namely, E° of (Cp^R)₂ZrCl₂ and the electron affinities of (Cp^R)₂Ni, Ru[$\eta^2\text{-OC(R)CHC(R)O}$]₃, and RO^{*}) give an opposite, albeit irregular, trend. Interestingly, XPS studies on (Cp^R)₂MCl₂, while not as extensive, are unusual in that yet another substituent trend is observed (Table 4). These discrepancies do not indicate that the electron-donating property of a substituent is determined by the method used to determine it—rather, it is the *interpretation* that is influenced by the technique. Thus, the electrochemical reduction of (Cp^R)₂ZrCl₂ is not dominated by inductive effects, and consequently, it is inappropriate to interpret changes in reduction potential as an indicator of the inductive effect of a substituent. Correspondingly, it indicates the importance of considering factors in addition to inductive effects when attempting to rationalize reactivity differences of metallocene complexes.

2.4. Other Spectroscopic Studies of Zirconocene Complexes. The lowest-energy UV/vis absorption bands of d⁰ metallocene complexes have been identified as ligand-to-metal charge transfer (LMCT) transitions, which correspond to the transfer of an electron from a cyclopentadienyl ligand-based HOMO to the metal-based LUMO.^{46,71} The energies of these transitions are influenced by the presence of substituents on the

(62) $\sigma_{\text{a(X)}} = \text{PP}(\text{MeX}) - \text{PP}(\text{MeH})$, where PP is the polarization parameter. See ref 60.

(63) The trimethylsilyl group has been described as possessing “dichotomous electron donor–acceptor properties. Under appropriate conditions proximate silicon groups can stabilize negative or positive charge and can strongly perturb the π -system in a variety of molecules.” See: Bassindale, A. R.; Taylor, P. G. In *The Chemistry of Organic Silicon Compounds*; Patai, S., Rappaport, Z., Eds.; John Wiley & Sons Ltd.: New York, 1989; Part 2, Chapter 12, pp 893–963.

(64) The relative importance of the polarization effect may be quantified by a dual parameter fit of the electrochemical data, $\Delta E^\circ_{\text{rel(X)Y}}/\text{mV} = a\sigma_{\text{meta(X)}} + b\sigma_{\text{a(X)}}$, which is characterized by the values $a = 700.5$ and $b = -64.2$, with $b/a = -0.09$; a fit that is not constrained to pass through the origin, i.e. $\Delta E^\circ_{\text{rel(X)Y}}/\text{mV} = a\sigma_{\text{meta(X)}} + b\sigma_{\text{a(X)}} + c$, is characterized by the values $a = 596.1$, $b = -58.9$, and $c = -5.4$.

(65) It is also worth noting that a methyl substituent exerts an effect of similar magnitude on ν_{CO} of other systems. For example, comparison of CpRe(CO)₃ and Cp^RRe(CO)₃ indicates a shift of ca. 3 cm^{−1} per methyl group. See: King, R. B.; Bisnette, M. B. *J. Organomet. Chem.* 1967, 8, 287–297.

(66) Bursten, B. E.; Callstrom, M. R.; Jolly, C. A.; Paquette, L. A.; Sivik, M. R.; Tucker, R. S.; Warchow, C. A. *Organometallics* 1994, 13, 127–133.

(67) Gassman, P. G.; Winter, C. H. *Organometallics* 1991, 10, 1592–1598.

(68) (a) Janiak, C.; Lange, K. C. H.; Versteeg, U.; Lentz, D.; Budzelaar, P. H. M. *Chem. Ber.* 1996, 129, 1517–1529. (b) Janiak, C.; Versteeg, U.; Lange, K. C. H.; Weimann, R.; Hahn, E. *J. Organomet. Chem.* 1995, 501, 219–234.

(69) Bühl, M.; Hopp, G.; von Philipsborn, W.; Beck, S.; Prosen, M.-H.; Rief, U.; Brintzinger, H.-H. *Organometallics* 1996, 15, 778–785.

(70) Böhme, U.; Thiele, K.-H.; Rufinska, A. *Z. Anorg. Allg. Chem.* 1994, 620, 1455–1462.

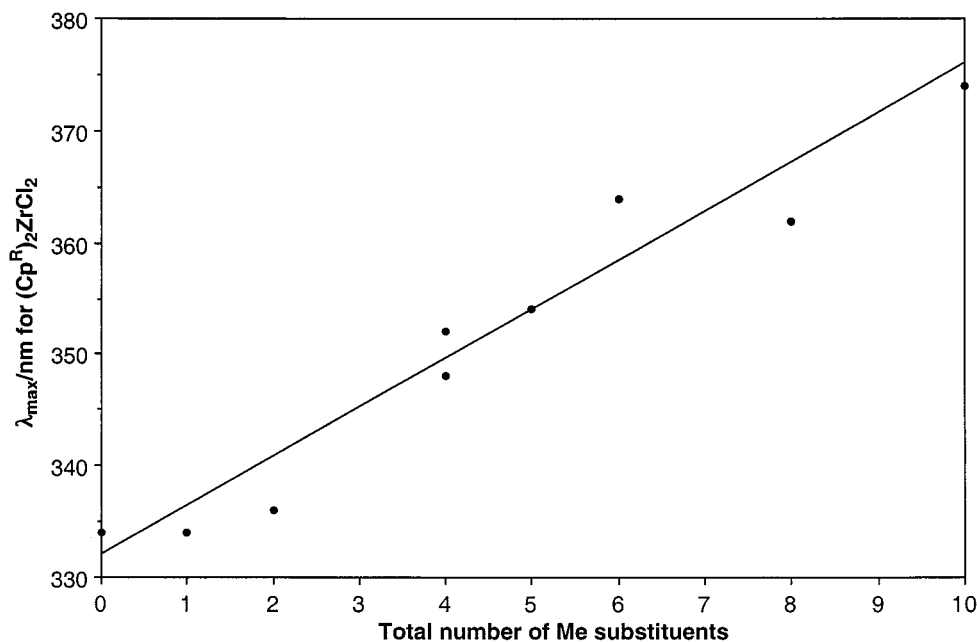


Figure 10. Influence of substituents on λ_{\max} of $(\text{Cp}^{\text{R}})_2\text{ZrCl}_2$.

cyclopentadienyl rings. For example, Grubbs has noted that the lowest-energy UV/vis band for titanocene complexes moves to lower energy as electron-donating substituents are added, and to higher energy with electron-withdrawing substituents.⁷²

We have recorded the UV/vis spectra of a large series of zirconocene dichloride complexes, as summarized in Table 2. In accord with previous observations that alkyl substituents result in shifts to longer wavelengths,⁷³ we have observed that multiple substitutions of the cyclopentadienyl rings of an extended series of $(\text{Cp}^{\text{Me}_x})(\text{Cp}^{\text{Me}_y})\text{ZrCl}_2$ derivatives result in an overall shift to longer wavelengths (Figure 10). However, by comparison to the IR spectroscopic study on the dicarbonyl counterparts, $(\text{Cp}^{\text{Me}_x})(\text{Cp}^{\text{Me}_y})\text{Zr}(\text{CO})_2$ (Figure 5), it is evident that the UV/vis spectroscopic data are more scattered. There are two possible reasons for the increased scatter. One reason is that the UV/vis absorption bands are broad and not as well-defined as the sharp ν_{CO} IR spectroscopic signals.⁷⁴ A second reason is that the energy of the UV/vis absorption band does not depend solely on the energy of a zirconium-based orbital. Specifically, the LMCT transition is influenced by the difference between the energy of the cyclopentadienyl-based HOMO and the energy of the zirconium-based LUMO, so that it does not per se provide a direct measure of the energy of the zirconium-based LUMO; consequently, it does not provide a direct indication of the “electron deficiency” of the zirconium center. In principle, the zirconium-based LUMO could be completely unaffected by the substituent, but the LMCT transition would still be influenced by the effect of a substituent on the energy of cyclopentadienyl-based HOMO. Thus, it is essential to supplement UV/vis

spectroscopic studies with calculations to ascertain the influence of a substituent on the energies of zirconium-based orbitals. For the present set of methylated derivatives, $(\text{Cp}^{\text{Me}_x})(\text{Cp}^{\text{Me}_y})\text{ZrCl}_2$, it is likely that the incremental incorporation of alkyl substituents results in a shift of the LMCT transition to lower energies due to the cyclopentadienyl-based HOMO being destabilized to a greater degree than is the zirconium-based LUMO.

Comparison of the lowest-energy UV/vis absorption bands for a large series of $(\text{Cp}^{\text{R}})_2\text{ZrCl}_2$ complexes with $\nu_{\text{CO}(\text{av})}$ for the corresponding dicarbonyl derivatives indicates that there is no general correlation,⁷⁵ although reasonable relationships exist for alkyl- and trimethylsilyl-substituted derivatives (Figure S1). The poor general correlation is in part a consequence of the fact that alkyl substituents and single-atom *ansa* bridges influence λ_{\max} in a similar way, whereas they influence ν_{CO} in opposite ways. This anomaly is due to the fact that $\nu_{\text{CO}(\text{av})}$ is directly dependent on the energy of a zirconium-based orbital, whereas the LMCT transition is not solely dependent on the energy of such an orbital, but also depends on the ligand-based HOMO. On this basis, we conclude that $\nu_{\text{CO}(\text{av})}$ provides a better and more direct experimental indication of the electronic impact of a cyclopentadienyl-substituent on a zirconium center than does the LMCT transition.

Another proposed measure of the electron-richness of a metal center is the $^1J_{\text{C-H}}$ coupling constant of transition-metal methyl complexes.^{76,77} Specifically, the $^1J_{\text{C-H}}$ coupling constant of a X-CH_3 derivative is highly dependent on the “Me⁻” versus “Me⁺” character of the methyl group due to a shift from sp^3 to sp^2 hybridization. Taking the $^1J_{\text{C-H}}$ coupling constant of 125 Hz for CH_4 as a point of reference, a polarity of the type $\text{X}^{\delta+}-\text{C}^{\delta-}$ results in a reduction of $^1J_{\text{C-H}}$ (to a value of 98 Hz for MeLi), whereas the opposite polarity $\text{X}^{\delta-}-\text{C}^{\delta+}$ results in an increase in $^1J_{\text{C-H}}$ (to a value of 166 Hz for “Me⁺”).⁷⁸

(71) (a) Mäkelä, N. I.; Knuutila, H. R.; Linnolahti, M.; Pakkanen, T. A. *J. Chem. Soc., Dalton Trans.* **2001**, 91–95. (b) Loukova, G. V.; Strelets, V. V. *Russ. Chem. Bull.* **2000**, 49, 1037–1039. (c) Loukova, G. V.; Strelets, V. V. *J. Organomet. Chem.* **2000**, 606, 203–206. (d) Wieser, U.; Schaper, F.; Brintzinger, H.-H.; Mäkelä, N. I.; Knuutila, H. R.; Leskelä, M. *Organometallics* **2002**, 21, 541–545.

(72) Finch, W. C.; Anslyn, E. V.; Grubbs, R. H. *J. Am. Chem. Soc.* **1988**, 110, 2406–2413.

(73) Specifically, the following values have been reported: Cp_2ZrCl_2 (333 nm), $(\text{Cp}^{\text{Me}_x})_2\text{ZrCl}_2$ (337 nm), $(\text{Cp}^{\text{Me}_y})_2\text{ZrCl}_2$ (350 nm). See ref 71d.

(74) In fact, we had to examine derivative spectra to identify λ_{\max} for several of these derivatives.

(75) Likewise, there is no correlation between E° and λ_{\max} .

(76) See, for example, ref 72 and (a) Bennett, B. L.; Hoerter, J. M.; Houllis, J. F.; Roddick, D. M. *Organometallics* **2000**, 19, 615–621. (b) Courtot, P.; Pichon, R.; Salaun, J. Y.; Toupet, L. *Can. J. Chem.* **1991**, 69, 661–672.

(77) Drago, R. S. *Physical Methods for Chemists*, 2nd ed.; Saunders: Orlando, FL, 1992; pp 252–257.

Table 5. ^1H and ^{13}C NMR Spectroscopic Data for the Zr-Me Groups of $(\text{Cp}^R)_2\text{ZrMe}_2$ Complexes

	δ (^1H)/ppm	δ (^{13}C)/ppm	$^1J_{\text{C-H}}$ /Hz
Cp_2ZrMe_2	-0.13	30.3	117.29
$(\text{Cp}^{\text{Me}_4})_2\text{ZrMe}_2$	-0.92	34.2	116.20
$\text{Cp}^{\text{Me}_2}_2\text{ZrMe}_2$	-0.56	36.1	116.48
$(\text{Cp}^{1,2-\text{Bu}^t})_2\text{ZrMe}_2$	0.16	30.6	116.98
$(\text{Cp}^{1,3-\text{Bu}^t})_2\text{ZrMe}_2$	0.18	32.2	115.89
$(\text{Cp}^{\text{Bu}^t-3,4-\text{Me}_2})_2\text{ZrMe}_2$	-0.16	32.9	116.86
$[\text{Me}_2\text{Si}(\text{C}_5\text{Me}_4)_2]\text{ZrMe}_2$	-0.51	34.1	116.20
$[\text{PhP}(\text{C}_5\text{Me}_4)_2]\text{ZrMe}_2$	-0.54, -0.56	34.9, 35.4	116.00, 115.00
$\{[\text{Me}_2\text{P}(\text{C}_5\text{Me}_4)_2]\text{ZrMe}_2\}$	-0.56	40.1	117.00
<i>rac</i> - $[\text{Me}_2\text{Si}(\text{C}_5\text{H}_2-2,4-\text{Bu}^t)_2]\text{ZrMe}_2$	0.33	33.9	116.20

Table 6. Influence of Single *Ansa* Carbon Bridges on E°_{rel} and $\nu_{\text{CO}(\text{av})}$ of the Parent Zirconocene System

	E°_{rel} /mV	$\nu_{\text{CO}(\text{av})}$ /cm $^{-1}$
Cp_2ZrX_2	0	1932
$[\text{H}_2\text{C}(\text{C}_5\text{H}_4)_2]\text{ZrX}_2$	65	-
$[\text{Me}_2\text{C}(\text{C}_5\text{H}_4)_2]\text{ZrX}_2$	57	1935
$[(\text{CH}_2\text{CH}_2)(\text{C}_5\text{H}_4)_2]\text{ZrX}_2$	25	1931
$[(\text{CH}_2\text{CH}_2\text{CH}_2)(\text{C}_5\text{H}_4)_2]\text{ZrX}_2$	-68	1929
$(\text{Cp}^{\text{Me}_6})_2\text{ZrX}_2$	-51	1927

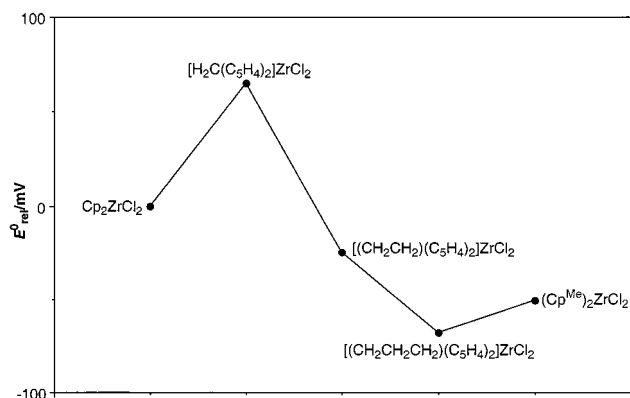
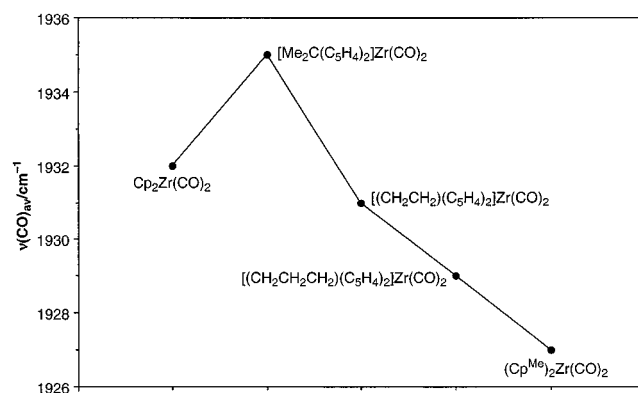
Electron-donating substituents attached to X are expected to lower its effective electronegativity and thus reduce $^1J_{\text{C-H}}$. While this is certainly true in the sense that Cp_2ZrMe_2 (117.3 Hz) has a larger $^1J_{\text{C-H}}$ coupling constant than that of $\text{Cp}^{\text{Me}_2}_2\text{ZrMe}_2$ (116.5 Hz), it is evident from the data listed in Table 5, which range from 115 to 117.3 Hz, that the changes are sufficiently small that such variations do not provide an accurate means for determining electronic substituent effects in this system.⁷⁹

3. Singly Bridged *Ansa* Zirconocene Complexes. Incorporation of a single *ansa* bridge in zirconocene complexes may exert an influence on both ν_{CO} of the dicarbonyls and E° of the dichlorides that is quite distinct from that expected by consideration of the unbridged system. Specifically, a single-atom (R_2C) linker has an opposite effect on ν_{CO} and E° to that of a methyl group, but as the length of the $(\text{CH}_2)_n$ bridge increases, the values approach those resulting from methyl substitution.

For example, consider the series of complexes $[(\text{R}_2\text{C})_n(\text{C}_5\text{H}_4)_2]\text{ZrCl}_2$ ($\text{R} = \text{H}, \text{Me}$). Whereas a methyl substituent on each cyclopentadienyl ligand causes a decrease of E° (i.e., inhibits reduction), a single CH_2 group results in a large increase (Table 6 and Figure 11). Specifically, the reduction potential for $(\text{Cp}^{\text{Me}_6})_2\text{ZrCl}_2$ is -51 mV, whereas that for $[\text{H}_2\text{C}(\text{C}_5\text{H}_4)_2]\text{ZrCl}_2$ is 65 mV. Likewise, the reduction potential for the $[\text{Me}_2\text{C}]$ -bridged counterpart $[\text{Me}_2\text{C}(\text{C}_5\text{H}_4)_2]\text{ZrCl}_2$ (57 mV) is also positive relative to $(\text{Cp}^{\text{Me}_6})_2\text{ZrCl}_2$. Thus, $[\text{R}_2\text{C}]$ bridges exert a net electron-withdrawing effect on a zirconocene center as judged by the ability to stabilize Zr^{III} relative to Zr^{IV} . Increasing the size of the bridge, however, causes a progressive reduction of E° such that the value for a trimethylene bridge (-68 mV) is comparable to that of $(\text{Cp}^{\text{Me}_6})_2\text{ZrCl}_2$ (-51 mV). A similar conclusion is obtained upon consideration of the average ν_{CO} values of the dicarbonyl complexes (Table 6 and Figure 12), which also shift to progressively lower values as the size of the bridge increases. Thus, in marked contrast to the substituent effects that are observed for unbridged zirconocene complexes, the electronic impact of an *ansa* bridge cannot simply be

(78) See data in Table 4 of ref 76a.

(79) Likewise, $^1J_{\text{C-H}}$ has been reported to be insensitive to substituent effects in complexes of the type L_2PtMe_2 . See, for example: Clark, H. C.; Manzer, L. E.; Ward, J. E. H. *Can. J. Chem.* **1974**, *52*, 1165–1170.

**Figure 11.** Influence of various carbon *ansa* bridges on E° of $(\text{Cp}^R)_2\text{ZrCl}_2$.**Figure 12.** Influence of various carbon *ansa* bridges on $\nu_{\text{CO}(\text{av})}$ of $(\text{Cp}^R)_2\text{Zr}(\text{CO})_2$.

interpreted on the basis of inductive, polarization, and solvation effects and indicates that displacement of the cyclopentadienyl rings from their natural positions now becomes an important factor.

A similar trend is observed for $[\text{Me}_2\text{Si}]$ bridges. Thus, a $[\text{Me}_2\text{Si}]$ bridge increases the reduction potential to a greater degree than would be predicted by incorporation of Me_3Si substituents on both rings. For example, the reduction potential of $[\text{Me}_2\text{Si}(\text{C}_5\text{H}_4)_2]\text{ZrCl}_2$ (118 mV) is more positive than that of $(\text{Cp}^{\text{TMS}})_2\text{ZrCl}_2$ (84 mV). A single $[\text{Me}_2\text{Si}]$ bridge also increases the reduction potential of the tetramethylated system, but the effect is not as great as that of Me_3Si substitution on both rings: $(\text{Cp}^{\text{Me}_4})_2\text{ZrCl}_2$ (-221 mV), $[\text{Me}_2\text{Si}(\text{C}_5\text{Me}_4)_2]\text{ZrCl}_2$ (-107 mV), and $(\text{Cp}^{\text{Me}_4\text{TMS}})_2\text{ZrCl}_2$ (-36 mV).

Consideration of the dicarbonyl complexes indicates that a $[\text{Me}_2\text{Si}]$ *ansa* bridge results in an increase in ν_{CO} (Table 2 and Figure S2). It is also significant that the net electron-withdrawing influence of a $[\text{Me}_2\text{Si}]$ *ansa* bridge, as judged by the impact on both ν_{CO} and E° is greater than that of a $[\text{Me}_2\text{C}]$ bridge. Since a $[\text{Me}_2\text{C}]$ bridge causes a greater displacement of the cyclopentadienyl rings from their natural positions than does a $[\text{Me}_2\text{Si}]$ bridge, it is evident that the greater electron-withdrawing influence of a $[\text{Me}_2\text{Si}]$ bridge is a result of the carbon-based $[\text{Me}_2\text{C}]$ bridge exerting a greater inductive effect which thereby partially counteracts the effect created by displacement of the rings. Thus, a $[\text{Me}_2\text{Si}]$ *ansa* bridge has a greater net electron-withdrawing influence than that of a $[\text{Me}_2\text{C}]$ bridge due to the silicon substituent exerting a poorer inductive effect.

As with the carbon-based linker, the electronic impact of a silylene bridge is diminished upon increasing the bridge size.

Thus, the $[\text{Me}_2\text{SiMe}_2\text{Si}]$ -bridged complex $[(\text{Me}_2\text{SiMe}_2\text{Si})(\text{C}_5\text{Me}_4)_2]\text{Zr}(\text{CO})_2$ (1904 cm^{-1}) exhibits a lower average ν_{CO} value than that of $[\text{Me}_2\text{Si}(\text{C}_5\text{Me}_4)_2]\text{Zr}(\text{CO})_2$ (1913 cm^{-1}) and is comparable to that of the unbridged counterpart $(\text{Cp}^{\text{Me}_4\text{TMS}})_2\text{Zr}(\text{CO})_2$ (1903 cm^{-1}). Likewise, the reduction potential for $[(\text{Me}_2\text{SiMe}_2\text{Si})(\text{C}_5\text{Me}_4)_2]\text{ZrCl}_2$ (-205 mV) is more negative than that for $[\text{Me}_2\text{Si}(\text{C}_5\text{Me}_4)_2]\text{ZrCl}_2$ (-107 mV).

There is very little information available concerning the electronic influence of [RP] bridges in zirconocene chemistry. Nevertheless, comparison of the ν_{CO} and E° values of $[\text{PhP}(\text{C}_5\text{Me}_4)_2]\text{Zr}(\text{CO})_2$ (1917 cm^{-1}) and $[\text{PhP}(\text{C}_5\text{Me}_4)_2]\text{ZrCl}_2$ (-4 mV) with those of $[\text{Me}_2\text{Si}(\text{C}_5\text{Me}_4)_2]\text{Zr}(\text{CO})_2$ (1913 cm^{-1}) and $[\text{Me}_2\text{Si}(\text{C}_5\text{Me}_4)_2]\text{ZrCl}_2$ (-107 mV) suggests that the [PhP] is marginally more electron-withdrawing than that of $[\text{Me}_2\text{Si}]$, as would be expected on the basis of the electronegativity differences of P (2.19) and Si (1.90).

The above data clearly indicate that $[\text{R}_2\text{C}]$, $[\text{R}_2\text{Si}]$, and [PhP] bridges behave as electron-withdrawing substituents in zirconocene chemistry, as judged by both ν_{CO} and E° values. In this regard, it is worth noting that the ability of the $[\text{Me}_2\text{Si}]$ bridge to create a ligand that decreases the electron richness of the metal center is an issue of some debate, stemming from an early prediction that it would actually create a more electron-rich metal center.¹⁷ The majority of studies, nevertheless, support the notion that a $[\text{Me}_2\text{Si}]$ bridge reduces electron density at a zirconium center. For example, XPS studies indicate that the $3d_{5/2}$ and $3d_{3/2}$ binding energies of $[\text{Me}_2\text{Si}(\text{C}_5\text{H}_4)_2]\text{ZrCl}_2$ (182.7 and 185.1 eV) are greater than those of Cp_2ZrCl_2 (182.0 and 184.4 eV).¹⁹ A similar conclusion has been derived by measurement of the gas phase appearance potentials of $[(\text{Cp}^{\text{R}})_2\text{ZrMe}]^+$ from $(\text{Cp}^{\text{R}})_2\text{ZrMe}_2$.¹⁹ Furthermore, gas-phase studies indicate that $\{[\text{Me}_2\text{Si}(\text{C}_5\text{H}_4)_2]\text{ZrMe}\}^+$ is more reactive than is $[\text{Cp}_2\text{ZrMe}]^+$ towards H_2 and C_2H_4 , and this result has been interpreted as implying the zirconium center in the former compound is more electrophilic.^{21,80}

To our knowledge, the only direct experimental study which suggests that the $[\text{Me}_2\text{Si}]$ bridge acts as an electron donor is that by Brintzinger, who employed a series of exchange studies to quantify the preference for a zirconocene center to coordinate methyl in preference to chloride.^{18,71c} Brintzinger's study indicates that incorporation of alkyl substituents on the cyclopentadienyl rings reduces the propensity of a zirconocene center to bind methyl in preference to chloride, thereby indicating that a more electron-deficient metal center favors coordination of the methyl group.⁸¹ On the basis of this criterion, the $[\text{Me}_2\text{Si}]$ bridge has been proposed to *increase* the electron density on a zirconocene center. This observation provides yet a further illustration of the difficulty associated with predicting the influence of cyclopentadienyl substituents and *ansa* bridges on the chemistry of metallocene derivatives, and how the interpretation is highly dependent on the system under consideration (e.g., Zr^{II} , Zr^{III} , Zr^{IV}) and the probe method.

(80) Richardson has used gas-phase electron-transfer equilibria data for ruthenocene derivatives to obtain a new scale for substituent effects in which an overall parameter (γ) is assigned to a cyclopentadienyl ligand rather than to individual substituents. The scale is anchored by $\gamma_{\text{Cp}} = 0$ and $\gamma_{\text{Cp}^{\text{R}}} = -1$, and on this scale the $\Sigma\gamma$ value for $[\text{Me}_2\text{Si}(\text{C}_5\text{H}_4)_2]$ is 0.16. See: Ryan, M. F.; Siedle, A. R.; Burk, M. J.; Richardson, D. E. *Organometallics* **1992**, *11*, 4231–4237.

(81) This interpretation is in accord with the general observation that the more electronegative metal preferentially binds the alkyl in alkyl/halide exchange between two metal centers. For example, Grubbs has reported that more electron-deficient centers favor methyl over chloride coordination in titanocene complexes. See ref 72.

4. Doubly Bridged *Ansa* Zirconocene Complexes. Doubly bridged *ansa* zirconocene complexes are not as common as their singly bridged counterparts.^{7,82} As such, the IR spectroscopic and electrochemical data are rather limited. Nevertheless, it is apparent that the *presence of a second ansa bridge has an electronic effect which is opposite to that introduced by a single bridge*. For example, whereas the single $[\text{Me}_2\text{Si}]$ bridge facilitates the reduction of $[\text{Me}_2\text{Si}(\text{C}_5\text{H}_4)_2]\text{ZrCl}_2$ ($E^\circ_{\text{rel}} = 118\text{ mV}$), the double $[\text{Me}_2\text{Si}]$ bridge inhibits the reduction of $[(\text{Me}_2\text{Si})_2(\text{C}_5\text{H}_3)_2]\text{ZrCl}_2$ ($E^\circ_{\text{rel}} = -47\text{ mV}$); for comparison purposes, unbridged trimethylsilyl substituted zirconocene complexes are characterized by reduction potentials in the range 50–121 mV (Table 2). Thus, it is evident that a double $[\text{Me}_2\text{Si}]$ bridge exerts an *electron-donating effect* on a zirconocene center, as judged by reduction potentials of the dichlorides.

A similar conclusion is derived by consideration of the $\nu_{\text{CO}(\text{av})}$ values of the dicarbonyl complexes. Specifically, the $\nu_{\text{CO}(\text{av})}$ values of $[1,1',2,2'-(\text{Me}_2\text{Si})_2(\text{C}_5\text{H}_2-4\text{Bu}^t)_2]\text{Zr}(\text{CO})_2$ (1915 cm^{-1}) and $[(1,1'-\text{Me}_2\text{Si})(2,2'-\text{Me}_2\text{C})(\text{C}_5\text{H}_2-4\text{Bu}^t)_2]\text{Zr}(\text{CO})_2$ (1916 cm^{-1}) are low compared to those of the related singly bridged complex, *meso*- $[\text{Me}_2\text{Si}(\text{C}_5\text{H}_3-3\text{Bu}^t)_2]\text{Zr}(\text{CO})_2$ (1925 cm^{-1}), and unbridged complexes $(\text{Cp}^{\text{Bu}^t})_2\text{Zr}(\text{CO})_2$ (1925 cm^{-1}), $(\text{Cp}^{1,3-\text{TMS}_2})_2\text{Zr}(\text{CO})_2$ (1924 cm^{-1}), and $(\text{Cp}^{1,2,4-\text{TMS}_3})_2\text{Zr}(\text{CO})_2$ (1923 cm^{-1}).

The observation that a double $[\text{Me}_2\text{Si}]$ bridge has a significant electron-donating effect, whereas a single $[\text{Me}_2\text{Si}]$ bridge exerts an electron-withdrawing effect, is most surprising. This is especially so when it is considered that Cp_2ZrCl_2 , $[\text{Me}_2\text{Si}(\text{C}_5\text{H}_4)_2]\text{ZrCl}_2$, and $[(\text{Me}_2\text{Si})_2(\text{C}_5\text{H}_3)_2]\text{ZrCl}_2$ exhibit a smooth variation in structure; for example, the $\text{Cp}_{\text{cent}}-\text{Zr}-\text{Cp}_{\text{cent}}$ angles (γ) progressively decrease (129.2° , 125.4° , and 120.6° , respectively), the tilt angles (τ) increase (1.4° , 2.8° , and 5.1° , respectively), and the range of Zr–C bond lengths ($\Delta(d_{\text{Zr}-\text{C}})$) increase (0.04 , 0.07 , and 0.16 \AA , respectively). Since there is a smooth variation in structure, it is unlikely that the opposite effects of the single and double *ansa* bridges can be rationalized by changes in $\text{Cp}_{\text{cent}}-\text{Zr}-\text{Cp}_{\text{cent}}$ angle and tilt angle. A possible explanation for the opposing effects of single and double $[\text{Me}_2\text{Si}]$ bridges, to be discussed in more detail below, resides with the fact that two bridges enforce a different conformation of the cyclopentadienyl rings. Specifically, as noted above, a single $[\text{Me}_2\text{Si}]$ bridge enforces a conformation in which an edge of each of the cyclopentadienyl rings faces the front of the metallocene (Class IV, Figure 1), whereas a double $[\text{Me}_2\text{Si}]$ bridge enforces a conformation in which a vertex of each of the cyclopentadienyl rings faces the front (Class III, Figure 1). The shift between “ η^3 -allyl-ene” and “ η^2 -ene-allyl” bonding

(82) For doubly bridged *ansa* metallocenes of the Group 4 elements, see refs 15, 38, and: (a) Royo, P. *New J. Chem.* **1997**, *21*, 791–796. (b) Cuenca, T.; Galakhov, M.; Royo, E.; Royo, P. *J. Organomet. Chem.* **1996**, *515*, 33–36. (c) Grossman, R. B.; Tsai, J. C.; Davis, W. M.; Gutierrez, A.; Buchwald, S. L. *Organometallics* **1994**, *13*, 3892–3896. (d) Weiss, K.; Neugebauer, U.; Blau, S.; Lang, H. *J. Organomet. Chem.* **1996**, *520*, 171–179. (e) Cano, A.; Cuenca, T.; Gomez-Sal, P.; Manzanero, A.; Royo, P. *J. Organomet. Chem.* **1996**, *526*, 227–235. (f) Halterman, R. L.; Tretyakov, A.; Combs, D.; Chang, J.; Khan, M. A. *Organometallics* **1997**, *16*, 3333–3339. (g) Miyake, S.; Bercaw, J. E. *J. Mol. Catal. A: Chem.* **1998**, *128*, 29–39. (h) Miyake, S.; Henling, L. M.; Bercaw, J. E. *Organometallics* **1998**, *17*, 5528–5533. (i) Fernandez, F. J.; Galakhov, M. V.; Royo, P. *J. Organomet. Chem.* **2000**, *594*, 147–153. (j) Warren, T. H.; Erker, G.; Fröhlich, R.; Wibbeling, B. *Organometallics* **2000**, *19*, 127–134. (k) Jung, J.; Noh, S. K.; Lee, D. H.; Park, S. K.; Kim, H. *J. Organomet. Chem.* **2000**, *595*, 147–152. (l) Peckham, T. J.; Nguyen, P.; Bourke, S. C.; Wang, Q.; Harrison, D. G.; Zoricak, P.; Russell, C.; Liable-Sands, L. M.; Rheingold, A. L.; Lough, A. J.; Manners, I. *Organometallics* **2001**, *20*, 3035–3043. (m) Dorer, B.; Proscen, M.-H.; Rief, U.; Brintzinger, H. H. *Organometallics* **1994**, *13*, 3868–3872.

Table 7. Selected Calculated Structural Parameters for $\text{Cp}^{\text{R}}_2\text{ZrCl}_2$ and $\text{Cp}^{\text{R}}_2\text{Zr}(\text{CO})_2$ ^a

	$\text{Cp}^{\text{R}}_2\text{ZrCl}_2$		$\text{Cp}^{\text{R}}_2\text{Zr}(\text{CO})_2$			
	α deg	γ deg	α deg	γ deg	$d(\text{Zr}-\text{C})$ Å	$d(\text{C}-\text{O})$ Å
Cp_2Zr	50 (54)	131 (129)	43	143	2.201	1.167
$(\text{Cp}^{\text{Me}})_2\text{Zr}$	54	130	44	144	2.198	1.167
$(\text{Cp}^{\text{Bu}^t})_2\text{Zr}$	59	129	47	144	2.190	1.169
$(\text{Cp}^{\text{TMS}})_2\text{Zr}$	54	128	44	143	2.195	1.169
Cp^*_2Zr	43 (44)	137 (137)	35	145	2.179	1.172
$[\text{Me}_2\text{C}(\text{C}_5\text{H}_4)_2]\text{Zr}$	71 (71)	116 (117)	71	121	2.220	1.165
$[\text{Me}_2\text{Si}(\text{C}_5\text{H}_4)_2]\text{Zr}$	58 (60)	126 (125)	58	132	2.215	1.166
$[(\text{Me}_2\text{Si})_2(\text{C}_5\text{H}_3)_2]\text{Zr}$	68 (70)	121 (121)	65	122	2.213	1.167

^a Where available, the experimental values for $\text{Cp}^{\text{R}}_2\text{ZrCl}_2$ are given in parentheses; structural references are given in Table 1.

modes for the singly and doubly bridged complexes, respectively, is proposed to be the origin of the different effects (vide infra).

5. Computational Study of Substituent and Ansa-Bridge Effects. The good correlation between ν_{CO} and Hammett σ_{meta} parameter for unbridged zirconocene $(\text{Cp}^{\text{R}})_2\text{Zr}(\text{CO})_2$ derivatives suggests that the principal impact of Me, Et, Prⁱ, Bu^t, and Me₃-Si substituents is via an inductive effect. Together with the ability to reconcile observed E° values for unbridged $(\text{Cp}^{\text{R}})_2\text{ZrCl}_2$ derivatives in terms of competing polarization and inductive effects, it is evident that the influence of a nonbridging substituent may generally be classified as an “electronic substituent effect”, that is, an effect that is not due to a structural change which is introduced by its bulk. In contrast, *ansa* bridges perturb the electronic properties of a zirconocene center by an additional mechanism resulting from the structural changes that are imposed by the various bridges, so that the observed modifications cannot merely be attributed to a simple “substituent effect”. To address this issue, we have performed DFT calculations on a series of zirconocene dicarbonyl⁸³ and dichloride⁸⁴ complexes.

Geometries were optimized for a selection of zirconocene dichlorides and dicarbonyls. The choice of complexes was made so that both the effect of alkyl substitution and the effect of introduction of single and double *ansa*-bridges could be explored. Key structural parameters are given in Table 7. The calculated values of α and γ for the dichlorides are in excellent agreement with the experimental values, where these exist. The Zr–C distances indicate that the carbon atoms at the narrow end of the metallocene wedge are closer to the metal and that the average Zr–C distance decreases on bending.

5.1 Electron Affinities of $(\text{Cp}^{\text{R}})_2\text{ZrCl}_2$. As a first approximation, the influence of a substituent on the reduction potential of $(\text{Cp}^{\text{R}})_2\text{ZrCl}_2$ was calculated by assuming that the trend would be similar to that of the gas-phase vertical electron affinity (EA) as defined by the difference in the electronic energies (E) of $(\text{Cp}^{\text{R}})_2\text{ZrCl}_2$ and $[(\text{Cp}^{\text{R}})_2\text{ZrCl}_2]^-$:

$$\text{EA} [(\text{Cp}^{\text{R}})_2\text{ZrCl}_2] = E [(\text{Cp}^{\text{R}})_2\text{ZrCl}_2] - E [(\text{Cp}^{\text{R}})_2\text{ZrCl}_2]^-$$

The calculated gas-phase electron affinities of $(\text{Cp}^{\text{R}})_2\text{ZrCl}_2$ follow the order, $\text{Cp}^{\text{TMS}2} \approx \text{Me}_2\text{Si}(\text{C}_5\text{H}_4)_2 > \text{Me}_2\text{C}(\text{C}_5\text{H}_4)_2 >$

(83) For previous Fenske–Hall^a and X-alpha^b calculations on $\text{Cp}_2\text{Zr}(\text{CO})_2$, see: (a) Lynn, M. A.; Bursten, B. E. *Inorg. Chim. Acta* **1995**, *229*, 437–443. (b) Casarin, M.; Ciliberto, E.; Gulino, A.; Fragala, I. *Organometallics* **1989**, *8*, 900–906.

(84) For recent calculations on $(\text{Cp}^{\text{R}})_2\text{ZrCl}_2$, see: Linnolahti, M.; Hirva, P.; Pakkanen, T. A. *J. Comput. Chem.* **2001**, *22*, 51–64.

Table 8. Comparison of Calculated Electron Affinities and Experimental Reduction Potentials of $(\text{Cp}^{\text{R}})_2\text{ZrCl}_2$

cmpd	calculated EA/eV	experimental $E^\circ_{\text{ref}}/\text{mV}$	$(\text{Cp}^{\text{R}})_2\text{ZrCl}_2$ LUMO/eV
Cp_2ZrCl_2	0.66	0	−2.77
$(\text{Cp}^{\text{Me}})_2\text{ZrCl}_2$	0.49	−51	−2.59
$(\text{Cp}^{\text{Bu}^t})_2\text{ZrCl}_2$	0.55	−14	−2.55
$(\text{Cp}^{\text{TMS}})_2\text{ZrCl}_2$	0.73	84	−2.74
$\text{Cp}^*_2\text{ZrCl}_2$	0.40	−244	−2.21
$[\text{Me}_2\text{C}(\text{C}_5\text{H}_4)_2]\text{ZrCl}_2$	0.67	78	−2.80
$[\text{Me}_2\text{Si}(\text{C}_5\text{H}_4)_2]\text{ZrCl}_2$	0.73	118	−2.83
$[(\text{Me}_2\text{Si})_2(\text{C}_5\text{H}_3)_2]\text{ZrCl}_2$	0.51	−47	−2.59

$\text{Cp}_2 > \text{Cp}^{\text{Bu}^t} > (\text{Me}_2\text{Si})_2(\text{C}_5\text{H}_3)_2 > \text{Cp}^{\text{Me}2} > \text{Cp}^*_2$, and are compared with the experimental reduction potentials in Table 8 and Figure S3, which indicate that the calculations reproduce the overall experimental trend. Thus, as found experimentally, *tert*-butyl is better at stabilizing the negative charge than Me, and trimethylsilyl is better than hydrogen. Furthermore, the singly bridged zirconocene dichlorides have higher electron affinities than their parent, whereas that of the doubly bridged example is lower. Although these gas-phase electron affinities are only one component of the thermodynamic cycle to which the electrode potentials can be related,⁸⁵ the calculations suggest that the trends in this component control to a large extent the variations in the electrode potentials.

5.2 ν_{CO} Infrared Stretching Frequencies of $(\text{Cp}^{\text{R}})_2\text{Zr}(\text{CO})_2$. The calculations indicate that the unbridged dicarbonyl complexes have significantly smaller interplanar-ring angles (α) than the corresponding dichlorides, whereas the *ansa*-bridged dicarbonyl and dichloride species have similar α values due to the rings being constrained by the presence of the bridge.⁸⁶ The calculated C–O distances of $(\text{Cp}^{\text{R}})_2\text{Zr}(\text{CO})_2$ show very little variation (1.165–1.172 Å). The Zr–C distances (2.18–2.22 Å) also vary little, but do so to a greater extent than the C–O distances (Table 7). Despite these small changes, the calculated $\nu_{\text{CO}(\text{av})}$ stretching frequencies vary over the range 1876–1918 cm^{-1} (Table 9). Furthermore, $\nu_{\text{CO}(\text{av})}$ is observed to correlate with the Zr–C distance, with $\nu(\text{CO})$ decreasing as the Zr–C bond becomes shorter.

The calculated $\nu_{\text{CO}(\text{av})}$ values for $(\text{Cp}^{\text{R}})_2\text{Zr}(\text{CO})_2$ follow the order, $\text{Me}_2\text{Si}(\text{C}_5\text{H}_4)_2 > \text{Me}_2\text{C}(\text{C}_5\text{H}_4)_2 > \text{Cp}_2 > (\text{Me}_2\text{Si})_2(\text{C}_5\text{H}_3)_2 \approx \text{Cp}^{\text{Me}2} > \text{Cp}^{\text{TMS}2} > \text{Cp}^{\text{Bu}^t} > \text{Cp}^*_2$. This order is in general agreement with the experimental data (Figure S4). However, it differs from the order of calculated electron affinities in that the Bu^t- and TMS-substituted zirconocenes now lie in the order of their inductive effects. The singly bridged zirconocene dicarbonyls have higher calculated $\nu_{\text{CO}(\text{av})}$ than the unsubstituted parent in contrast to the doubly bridged which is calculated to have a lower $\nu_{\text{CO}(\text{av})}$. Thus, in relation to structure, electron affinities, and carbonyl stretching frequencies, the calculations reproduce the trends and anomalies of the experimental data very well. We therefore have confidence in examining the details

(85) Specifically, the calculations do not take into account either the gas-phase relaxation energy of $[(\text{Cp}^{\text{R}})_2\text{ZrCl}_2]^-$ or the differing solvation of $(\text{Cp}^{\text{R}})_2\text{ZrCl}_2$ and $[(\text{Cp}^{\text{R}})_2\text{ZrCl}_2]^-$.

(86) By comparison with the dichlorides, there are relatively few experimentally determined structures for the dicarbonyl derivatives, $(\text{Cp}^{\text{R}})_2\text{Zr}(\text{CO})_2$, which include: $\text{Cp}_2\text{Zr}(\text{CO})_2$,^a $\text{Cp}^*_2\text{Zr}(\text{CO})_2$,^b $(\text{ind})_2\text{Zr}(\text{CO})_2$,^c and $[\text{PhP}(\text{C}_5\text{Me}_4)_2]\text{Zr}(\text{CO})_2$.^d (a) Atwood, J. L.; Rodgers, R. D.; Hunter, W. E.; Floriani, C.; Fachinetti, G.; Chiesi-Villa, A. *Inorg. Chem.* **1980**, *19*, 3812–3817. (b) Sikora, D. J.; Rausch, M. D.; Rogers, R. D.; Atwood, J. L. *J. Am. Chem. Soc.* **1981**, *103*, 1265–1267. (c) Rausch, M. D.; Moriarty, K. J.; Atwood, J. L.; Hunter, W. E.; Samuel, E. J. *Organomet. Chem.* **1987**, *327*, 39–54. (d) Shin, J. H.; Hascall, T.; Parkin, G. *Organometallics* **1999**, *18*, 6–9.

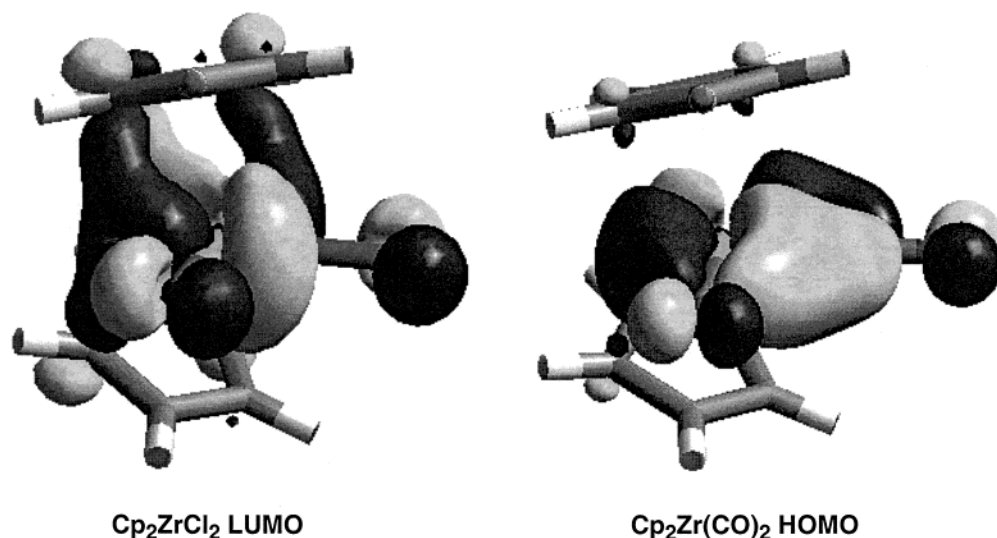


Figure 13. Iso-surfaces for the a_1 LUMO of Cp_2ZrCl_2 and the a_1 HOMO of $\text{Cp}_2\text{Zr}(\text{CO})_2$.

Table 9. Comparison of Calculated and Experimental $\nu(\text{CO})_{\text{av}}$ Values for $(\text{Cp}^{\text{R}})_2\text{Zr}(\text{CO})_2$ and Energies of the $3a_1$ HOMO of $[\text{Cp}^{\text{R}}_2\text{Zr}]$ and $[\text{Cp}_2\text{Zr}]$ with Geometries Corresponding to the Optimized Structures of $(\text{Cp}^{\text{R}})_2\text{Zr}(\text{CO})_2$; the Difference in These Two $3a_1$ Energies Is a Measure of the Substituent Effect

cmpd	calculated $\nu(\text{CO})_{\text{av}}/\text{cm}^{-1}$	experimental $\nu(\text{CO})_{\text{av}}/\text{cm}^{-1}$	$(\text{Cp}^{\text{R}})_2\text{Zr}(\text{CO})_2$ HOMO/eV	$[\text{Cp}^{\text{R}}_2\text{Zr}]$ $3a_1/\text{eV}$	$[\text{Cp}_2\text{Zr}]_{\text{equiv geom}}$ $3a_1/\text{eV}$	subst effect $\Delta 3a_1/\text{eV}$
$\text{Cp}_2\text{Zr}(\text{CO})_2$	1910.0	1932.0	-3.84	-2.49	-2.49	0.00
$(\text{Cp}^{\text{Me}})_2\text{Zr}(\text{CO})_2$	1906.5	1926.5	-3.72	-2.39	-2.52	0.13
$(\text{Cp}^{\text{Bu}})_2\text{Zr}(\text{CO})_2$	1893.0	1925.0	-3.69	-2.33	-2.55	0.22
$(\text{Cp}^{\text{TMS}})_2\text{Zr}(\text{CO})_2$	1896.5	1929.0	-3.79	-2.45	-2.52	0.07
$\text{Cp}^*\text{Zr}(\text{CO})_2$	1875.5	1899.5	-3.35	-2.12	-2.56	0.44
$[\text{Me}_2\text{C}(\text{C}_5\text{H}_4)_2]\text{Zr}(\text{CO})_2$	1916.0	1935.0	-3.80	-2.44	-2.47	0.03
$[\text{Me}_2\text{Si}(\text{C}_5\text{H}_4)_2]\text{Zr}(\text{CO})_2$	1917.5	1939.5	-3.86	-2.60	-2.50	-0.10
$[(\text{Me}_2\text{Si})_2(\text{C}_5\text{H}_3)_2]\text{Zr}(\text{CO})_2$	1907.0	—	-3.79	-2.26	-2.18	-0.08

of the calculated electronic structure to understand the origin of the variations.

5.3. Electronic Structure of Zirconocene Complexes and the Origin of the Electronic Influence of Ansa Bridges. The generic electronic structure of a bent metallocene unit is well understood, and has been so for decades,^{87,88} but detailed examination of particular cases is still rewarding in terms of an understanding of structure and reactivity.⁸⁹ The highest symmetry for the bent metallocene unit is C_{2v} ; with lower symmetry the frontier orbitals are little changed and so we will use the C_{2v} symmetry labels here. The key orbital in determining both the electron affinity of $(\text{Cp}^{\text{R}})_2\text{ZrCl}_2$ and $\nu_{\text{CO}(\text{av})}$ of $(\text{Cp}^{\text{R}})_2\text{Zr}(\text{CO})_2$ is of a_1 symmetry, derived from the $3a_1$ orbital of the zirconocene fragment (Figures 13 and 14).

The a_1 orbital in $(\text{Cp}^{\text{R}})_2\text{ZrCl}_2$ is unoccupied, is the LUMO of the molecule, and is the orbital which is half occupied in $[(\text{Cp}^{\text{R}})_2\text{ZrCl}_2]^-$. This a_1 orbital has an antibonding interaction with the two Cl ligands, but has the capacity to back-bond to the rings, as illustrated in Figures 13 and 14. Despite the fact that it is the a_1 LUMO in neutral $(\text{Cp}^{\text{R}})_2\text{ZrCl}_2$ which becomes occupied upon adding an electron to the system, the energy of

this orbital does not track the calculated electron affinities exactly, as illustrated by the poor correlation between calculated EA and the LUMO energy (Figure S5). Thus, although the LUMO energy is a significant factor, it is evident that other factors, such as the polarizability of the substituent groups, influence the electron affinity.

For the d^2 dicarbonyl series, the HOMO is an a_1 orbital that is mainly a mixture of metal d orbitals and CO π^* orbitals (Figures 13 and 14). Interaction with the rings is reduced, however, compared to the dichlorides because of the preferential strong back-donation to the π^* orbitals of the two CO groups. Fragment calculations show that $\nu_{\text{CO}(\text{av})}$ is directly related to the metal contribution to the HOMO, and except in the case of $\text{Cp}^*\text{Zr}(\text{CO})_2$, the fragment contribution is almost exclusively from the $3a_1$ orbital. However, for $\text{Cp}^*\text{Zr}(\text{CO})_2$, in which the metallocene fragment is less bent than in other $(\text{Cp}^{\text{R}})_2\text{Zr}(\text{CO})_2$ derivatives, the $3a_1$ and $4a_1$ orbitals lie close in energy so that both fragment orbitals contribute to the HOMO of $\text{Cp}^*\text{Zr}(\text{CO})_2$. It is also the case that the fragment contribution to the HOMO of $(\text{Cp}^{\text{R}})_2\text{Zr}(\text{CO})_2$ is dominated by the fragment energy rather than the $3a_1-\pi^*$ overlap, with back-bonding to the carbonyl ligands being favored by a high-energy $3a_1$ orbital. Thus, further analysis of the underlying causes of the energies of the fragment frontier orbitals is called for to be able to determine the influence of a ring substituent on $\nu_{\text{CO}(\text{av})}$.

To separate the effect of varying the ring geometry from the effect of substituents, we calculated the energy of a $[\text{Cp}_2\text{Zr}]$ fragment with no substituents, but with the optimized geometry

(87) Green, J. C.; Green, M. L. H.; Prout, C. K. *J. Chem. Soc., Chem. Commun.* **1972**, 421–422.

(88) Lauher, J. W.; Hoffmann, R. *J. Am. Chem. Soc.* **1976**, *98*, 1729–1742 and references therein.

(89) (a) Green, J. C.; Jardine, C. N. *J. Chem. Soc., Dalton Trans.* **1998**, 1057–1061. (b) Green, J. C.; Scottow, A. *New J. Chem.* **1999**, *23*, 651–655. (c) Green, J. C.; Jardine, C. N. *J. Chem. Soc., Dalton Trans.* **1999**, 3767–3770. (d) Green, J. C.; Jardine, C. N. *J. Chem. Soc., Dalton Trans.* **2001**, 274–276. (e) Ashworth, N. J.; Conway, S. L. J.; Green, J. C.; Green, M. L. H. *J. Organomet. Chem.* **2000**, *609*, 83–88.

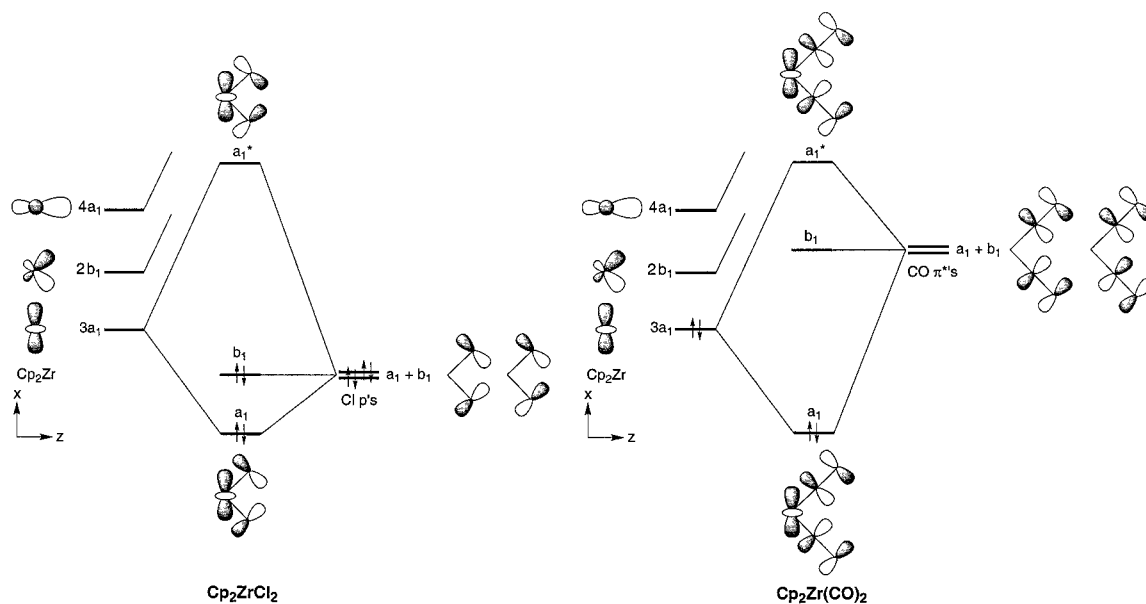


Figure 14. π -Interactions in the metallocene plane of Cp_2ZrCl_2 and $\text{Cp}_2\text{Zr}(\text{CO})_2$, emphasizing the role of the $3a_1$ orbital. The $2b_1$ and $4a_1$ orbitals primarily participate in sigma interactions with the Cl and CO ligands.

of the metallocene unit in each of eight zirconocene dicarbonyls, $(\text{Cp}^R)_2\text{Zr}(\text{CO})_2$. The energies of the resulting $3a_1$ HOMOs are given in Table 9. For all except that corresponding to the geometry of the doubly bridged $[\text{Me}_2\text{Si}]$ derivative $(\text{Me}_2\text{Si})_2(\text{C}_5\text{H}_3)_2\text{Zr}(\text{CO})_2$, which will be discussed in more detail below, the energy of the $[\text{Cp}_2\text{Zr}]$ $3a_1$ HOMO is relatively insensitive to the zirconocene geometry (a range of 0.09 eV).⁹⁰ The relative insensitivity of the HOMO energy to zirconocene geometry indicates that the electronic effect of an unbridged substituent is principally a result of inductive effects, with perturbations due to structural distortions being minor. A similar conclusion has been made by XPS studies and calculations on titanocene complexes.⁶⁶

The difference between the energy of the $3a_1$ orbital in $[(\text{Cp}^R)_2\text{Zr}]$ and that of $[\text{Cp}_2\text{Zr}]$ with the identical geometry ($\Delta 3a_1$) provides a direct indication of the effect of a substituent in the absence of conformational changes and interplanar angle variations of the cyclopentadienyl rings. For the unbridged series, all substituents have a destabilizing effect on the $3a_1$ orbital energy of $[(\text{Cp}^R)_2\text{Zr}]$ in the order expected on the basis of their inductive effects: $\text{Cp}^{\text{TMS}} < \text{Cp}^{\text{Me}} < \text{Cp}^{\text{Bu}^t} < \text{Cp}^*$. However, this influence is modulated if the substituent is part of an *ansa* bridge. For example, the substituent effect for $[(\text{Cp}^{\text{Me}})_2\text{Zr}]$ is 0.13 eV, whereas that for $\{[\text{Me}_2\text{C}(\text{C}_5\text{H}_4)_2]\text{Zr}\}$ is only 0.03 eV. Furthermore, a Me_3Si substituent has a destabilizing effect on the $3a_1$ orbital in $[(\text{Cp}^{\text{TMS}})_2\text{Zr}]$ (0.07 eV), but a single $[\text{Me}_2\text{Si}]$ bridge has a stabilizing effect (-0.10 eV). The double $[\text{Me}_2\text{Si}]$ bridge in $\{[(\text{Me}_2\text{Si})_2(\text{C}_5\text{H}_3)_2]\text{Zr}\}$ also exerts a stabilizing effect (-0.08 eV) relative to that of $[\text{Cp}_2\text{Zr}]$ with the identical geometry.

Thus, in each case studied, the *ansa* bridge exerts a stabilizing effect on the $3a_1$ orbital relative to the same zirconocene structure in the absence of a bridge. This stabilization, which may be interpreted in terms of an electron-withdrawing effect, is in contrast to the electron-releasing influence of the non-bridged substituents. A possible explanation for the modulation

of the inductive effect, due to the substituent being a component of an *ansa* bridge, resides with the fact that the energy of the $3a_1$ orbital is dependent on the combined acceptor power of the two cyclopentadienyl rings.

The $3a_1$ orbital of $[\text{Cp}_2\text{Zr}]$ resembles a d_{x^2} orbital pointing across the metallocene wedge (Figures 14 and 15). While this orbital is largely metal-based, there is also a contribution from the cyclopentadienyl ligands. The cyclopentadienyl ligand acceptor orbital is the a_1 symmetry adapted combination of the two cyclopentadienyl e_2 δ -character orbitals, and the interaction represents δ -back-donation from the metal to the ligand, as illustrated in Figure 15 for two conformations of the cyclopentadienyl ligands. The cyclopentadienyl ligand acceptor orbital becomes bonding between the two rings as the metallocene is bent and the atoms become closer. As such, this interaction would be promoted by a reduction in $\text{Cp}_{\text{cent}}-\text{Zr}-\text{Cp}_{\text{cent}}$ angle (γ) and an increase in tilt angle (τ), the latter of which corresponds to a shift towards η^3 -coordination with the *ipso* and two neighboring carbon atoms being closer to the metal than the two distal carbons (Figure 3). It should also be noted that a single-atom *ansa* bridge enforces a conformation in which two vertices of the cyclopentadienyl ring point towards the rear of the metallocene wedge (Class IV, Figure 1), and thus are closest together; in the absence of a bridge, such a conformation is normally unstable because of interannular interactions. In addition to the distance dependence of the inter-ring interaction, the interaction is also facilitated by the bridging atoms, as illustrated by comparison of the a_1 acceptor orbitals of the $[\text{Cp}_2]$, $[\text{Me}_2\text{C}(\text{C}_5\text{H}_4)_2]$ and $[\text{Me}_2\text{Si}(\text{C}_5\text{H}_4)_2]$ fragments (Figure 16). Stabilization of the combined ligand acceptor orbital by the bridging atom would serve to enhance back-bonding from the zirconium $3a_1$ orbital, as illustrated schematically in (Figure 17), and hence subsequently stabilize the metal-centered orbital. Thus, the electron-withdrawing effect of the $[\text{Me}_2\text{C}]$ and $[\text{Me}_2\text{Si}]$ *ansa*-bridges, as revealed experimentally by both the electrode potential and the carbonyl frequency data, can be attributed to the stabilization of the cyclopentadienyl ligand

(90) The $3a_1$ orbital does, nevertheless, tend to rise slightly in energy with increased bending of the metallocene unit.

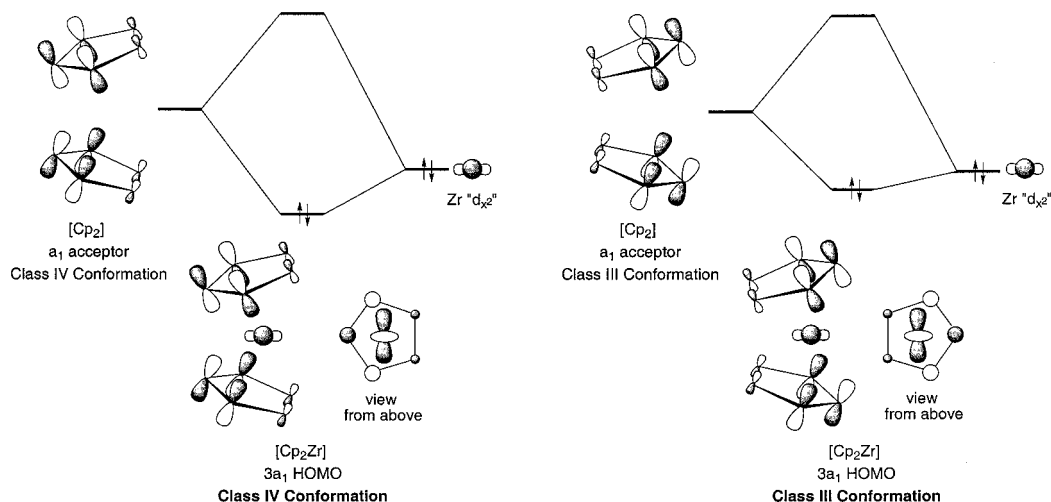


Figure 15. Back-bonding interaction between the filled $d_{x^2-y^2}$ orbital and the cyclopentadienyl ligand acceptor orbital for two conformations of the cyclopentadienyl ligands.

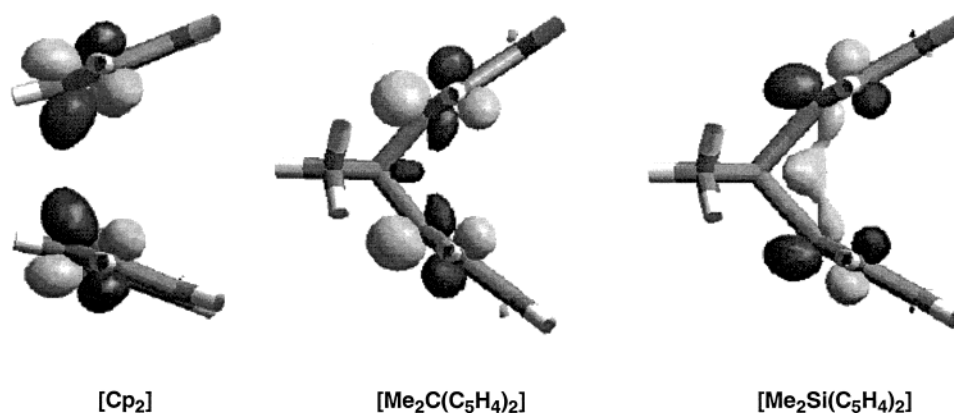


Figure 16. Iso-surfaces for the a_1 LUMOs of the $[\text{Cp}_2]$, $[\text{Me}_2\text{C}(\text{C}_5\text{H}_4)_2]$ and $[\text{Me}_2\text{Si}(\text{C}_5\text{H}_4)_2]$ fragments.

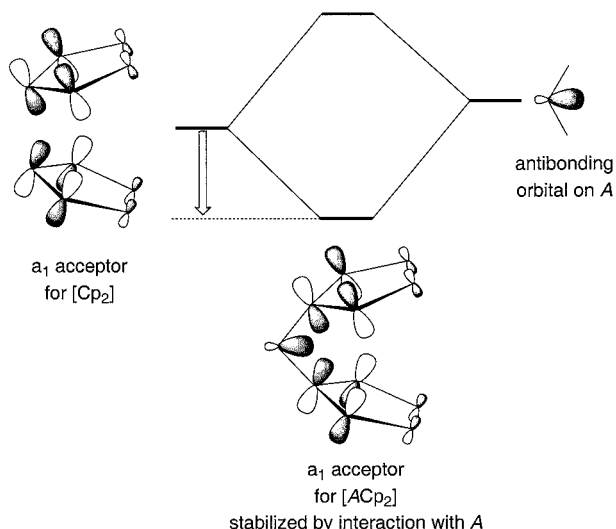


Figure 17. Stabilization of the combined cyclopentadienyl ligand a_1 acceptor orbital by the bridging atom.

acceptor orbital which subsequently enhances back-donation from the metal.

Whereas the electronic influence of a single *ansa* bridge can be rationalized in terms of a modified substituent effect, the electron-donating influence of a double $[\text{Me}_2\text{Si}]$ bridge cannot. The electron-donating character of the $[(\text{Me}_2\text{Si})_2(\text{C}_5\text{H}_3)_2]$ ligand

is manifested by a particularly high energy for the $3a_1$ orbital of the $\{[(\text{Me}_2\text{Si})_2(\text{C}_5\text{H}_3)_2]\text{Zr}\}$ fragment. In this regard, calculations on the $[\text{Cp}_2\text{Zr}]$ entity indicate that the energy of the $3a_1$ orbital of $[(\text{Me}_2\text{Si})_2(\text{C}_5\text{H}_3)_2]\text{Zr}(\text{CO})_2$ (-2.18 eV) is substantially higher than for those with the geometries corresponding to all other derivatives (-2.47 to -2.56 eV). Since the energies of the $3a_1$ orbital in $\{[(\text{Me}_2\text{Si})_2(\text{C}_5\text{H}_3)_2]\text{Zr}\}$ (-2.26 eV) and $[\text{Cp}_2\text{Zr}]$ (-2.18 eV) with the same geometry are similar, it is evident that the particularly high value for $\{[(\text{Me}_2\text{Si})_2(\text{C}_5\text{H}_3)_2]\text{Zr}\}$ relative to other zirconocenes is a result of the structure imposed by the double $[\text{Me}_2\text{Si}]$ *ansa* bridge. However, the high energy of the $3a_1$ orbital is *not* a result of an unusual inter-ring angle (α). For example, the inter-ring angle for $[(\text{Me}_2\text{Si})_2(\text{C}_5\text{H}_3)_2]\text{Zr}(\text{CO})_2$ (65°) is intermediate between those of $[\text{Me}_2\text{Si}(\text{C}_5\text{H}_4)_2]\text{Zr}(\text{CO})_2$ (58°) and $[\text{Me}_2\text{C}(\text{C}_5\text{H}_4)_2]\text{Zr}(\text{CO})_2$ (71°), but the ligands in the last two complexes exert an electron-withdrawing effect that stabilizes the metal centered orbital.

Since the inter-ring angle itself does not have a significant impact on the HOMO energy of $[\text{Cp}_2\text{Zr}]$, we propose that it is the *conformation* of the two cyclopentadienyl ligands, enforced by the double *ansa* bridge, which is responsible for the enhanced electron-donating characteristics. In this respect, the ring orientations of $[(\text{Me}_2\text{Si})_2(\text{C}_5\text{H}_3)_2]\text{Zr}(\text{CO})_2$ differ from those of all the other compounds studied here in that it belongs to Class III (Figure 1). This conformation (i.e., an eclipsed geometry in

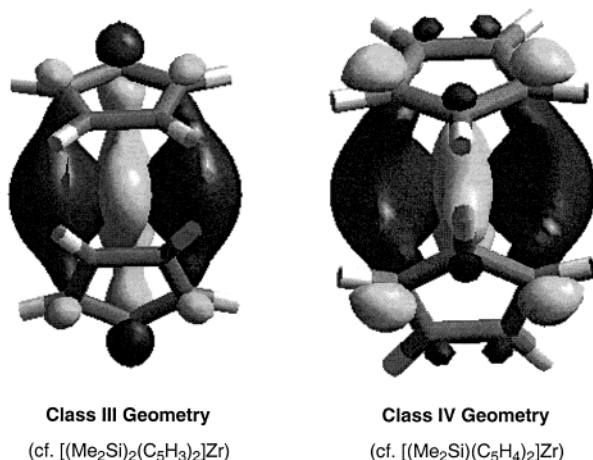


Figure 18. Iso-surfaces for the 3a₁ HOMO of [Cp₂Zr] with Class III and IV orientations of the cyclopentadienyl rings.

which four carbon atoms are located at the narrow rear of the metallocene wedge) is uncommon but is mandated for [(Me₂-Si)₂(C₅H₃)₂]Zr(CO)₂ by the presence of the double *ansa* bridge.

The conformation of the cyclopentadienyl rings exerts an electronic influence by affecting the energy and character of the frontier orbitals. Thus, the 3a₁ orbital of [Cp₂Zr] with a Class IV conformation possesses 65% d character, whereas that with a Class III conformation possesses 73% d character and hence a relatively higher energy. The energy and composition of the 3a₁ orbital of [Cp₂Zr] varies with conformation due to the fact that overlap with the cyclopentadienyl ligand orbitals is dependent upon the conformation of the rings (Figure 15). Iso-surfaces of the 3a₁ orbital for the Class III and IV [Cp₂Zr] fragments (Figure 18) show that the former has contributions from the carbons at the wide end of the wedge and the latter from the narrow part. The relative overlaps are controlled by the nodal surface of the d_{x²} orbital, as illustrated in Figure 19. Furthermore, since the carbons at the narrow end of the wedge are closer to the metal than the others, back-donation to the cyclopentadienyl ligands in a Class IV structure is greater than that in a Class III structure (Figures 15 and 19).

As a result of the reduced back-bonding to the cyclopentadienyl rings for a Class III structure, the 3a₁ orbital for a Class III structure possesses greater metal character than one with a Class IV structure. Consequently, the 3a₁ orbital for a Class III structure retains a higher energy and is therefore capable of more effective back-donation with the carbonyl ligands. The unexpectedly high electron-donating property of the [(Me₂Si)₂(C₅H₃)₂] ligand may, therefore, be rationalized as a result of the cyclopentadienyl conformation enforced by the double [Me₂-Si] *ansa* bridge which minimizes back-bonding from the metal.

Conclusions

In addition to steric factors, recognition of the electronic influence of *ansa* bridges is essential for understanding the way that such groups may modify the applications of metallocenes in polymerization catalysis and organic syntheses. The electronic influence of *ansa*-bridged substituents on a zirconocene center has been ascertained by using a combination of IR spectroscopic, electrochemical, and computational methods. With respect to IR spectroscopy, the average of the symmetric and asymmetric stretches ($\nu_{\text{CO(av)}}$) of a large series of dicarbonyl complexes

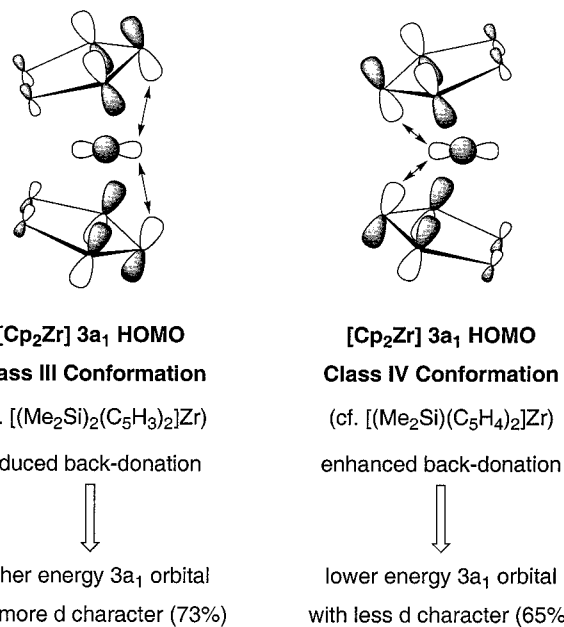


Figure 19. Enhanced interaction between filled d_{x²} orbital and cyclopentadienyl acceptor orbital for the Class IV conformation results in a lower energy 3a₁ orbital, which subsequently minimizes back-bonding to the carbonyl ligands.

(Cp^R)₂Zr(CO)₂ has been used as a probe of the electronic influence of a cyclopentadienyl ring substituent. For unbridged substituents (Me, Et, Prⁱ, Bu^t, SiMe₃), $\Delta\nu_{\text{CO(av)}}$ on a per substituent basis correlates well with Hammett σ_{meta} parameters, thereby indicating that the influence of these substituents is via a simple inductive effect. In contrast, the reduction potentials (E°) of the corresponding dichloride complexes (Cp^R)₂ZrCl₂ do not correlate well with Hammett σ_{meta} parameters, thereby suggesting that factors other than the substituent inductive effect also influence E° . Two such factors that play a role due to the differing charge of (Cp^R)₂ZrCl₂ and [(Cp^R)₂ZrCl₂]⁻ are polarization and solvation. Trimethylsilyl substituents influence E° in an unusual manner. Thus, a single Me₃Si group on each ring causes a significant increase in E° , but further substitutions have little additional impact, and a leveling effect is observed. Since E° values are influenced by several factors, they do not necessarily provide a direct indication of the electronic influence of a substituent on a zirconium center; $\nu_{\text{CO(av)}}$ is therefore considered the better of the two measurements for assessing the electronic perturbation of the zirconium center in zirconocene complexes.

With respect to the electronic influence of *ansa*-bridged substituents, the following conclusions may be made:

(i) *Ansa* bridges with single-atom linkers, for example, [Me₂C] and [Me₂Si], exert a net electron-withdrawing effect as judged by both $\nu_{\text{CO(av)}}$ and E°_{rel} values. Calculations demonstrate that the electron-withdrawing effect of the [Me₂C] and [Me₂Si] *ansa* bridges is a result of stabilization of the cyclopentadienyl ligand acceptor orbital, which subsequently enhances back-donation from the metal to the cyclopentadienyl ligands. Stabilization of the cyclopentadienyl ligand acceptor orbital is a result of both (a) geometrical changes, that is, a reduction in Cp_{cent}-Zr-Cp_{cent} angle (γ) and an increase in tilt angle (τ) which cause the *ipso* and two neighboring carbon atoms to be closer to the metal than the two distal carbon atoms, and (b) the orbital involvement by atoms of the *ansa* bridge.

Table 10. Crystal, Intensity Collection, and Refinement Data

	[H ₂ C(C ₅ H ₄) ₂]ZrCl ₂	[H ₂ C(C ₅ H ₄) ₂]ZrI ₂	[(CH ₂ CH ₂)(C ₅ H ₄) ₂]ZrCl ₂
lattice	monoclinic	orthorhombic	monoclinic
formula	C ₁₁ H ₁₀ Cl ₂ Zr	C ₁₁ H ₁₀ I ₂ Zr	C ₁₂ H ₁₂ Cl ₂ Zr
formula weight	304.31	487.21	318.34
space group	C2/c	Cmcm	C2/c
a/Å	12.292(1)	12.469(1)	13.411(12)
b/Å	11.147(1)	11.479(1)	8.227(7)
c/Å	8.650(1)	8.691(1)	12.280(11)
α/deg	90	90	90
β/deg	111.110(1)	90	119.86(1)
γ/deg	90	90	90
V/Å ³	1105.7(2)	1243.9(2)	1175(2)
Z	4	4	4
temperature (K)	233	233	233
radiation (λ, Å)	0.71073	0.71073	0.71073
ρ (calcd), g cm ⁻³	1.828	2.602	1.800
μ (Mo Kα), mm ⁻¹	1.432	5.808	1.352
θ max, deg	28.04	28.19	28.34
no. of data	1254	798	1328
no. of parameters	66	43	125
R1	0.0188	0.0248	0.0283
wR2	0.0503	0.0570	0.0730
GOF	1.090	1.135	1.026

(ii) A [Me₂Si] bridge has a greater electron-withdrawing effect than that of a [Me₂C] bridge. Since a [Me₂C] bridge causes a greater displacement of the cyclopentadienyl rings from their natural positions than does a [Me₂Si] bridge, the greater electron-withdrawing influence of a [Me₂Si] bridge is proposed to be a result of the [Me₂C] bridge exerting a greater inductive effect which thereby partially counteracts the effect created by displacement of the rings.

(iii) The electron-withdrawing effect of the *ansa* bridge is diminished upon increasing its length. Indeed, with a linker comprising a three-carbon chain, the [CH₂CH₂CH₂] *ansa* bridge becomes electron-donating as judged by both $\nu_{\text{CO(av)}}$ of [(CH₂-CH₂CH₂)(C₅H₄)₂]Zr(CO)₂ and E°_{rel} of [(CH₂CH₂CH₂)(C₅H₄)₂]ZrCl₂.

(iv) In contrast to the electron-withdrawing effect observed for a single [Me₂Si] *ansa* bridge, a pair of vicinal [Me₂Si] *ansa* bridges rather surprisingly exerts an electron-donating effect relative to the single bridge. An explanation for the opposing effects of single and double [Me₂Si] bridges resides with the fact that the single and double bridges enforce different conformations of the cyclopentadienyl rings, that is, a single [Me₂Si] bridge enforces an “ η^3 -allyl-ene” type coordination mode, whereas a double [Me₂Si] bridge enforces an “ η^2 -ene-allyl” type coordination mode. The calculations demonstrate that the conformation enforced by the double *ansa* bridge reduces back-donation from the metal-centered d orbital, thus resulting in the unexpectedly high electron-donating property of the [(Me₂Si)₂(C₅H₃)₂] ligand.

Finally, it is important to emphasize that *interpretations* pertaining to the electron-donating or -withdrawing properties of cyclopentadienyl ring substituents is highly dependent upon the specific system and the probe method used to investigate it. However, more important than assigning labels such as “electron-donating” or “electron-withdrawing” to a substituent, is the influence of the substituent on the *chemistry* of a system. The methods used in the present study address cyclopentadienyl ligand effects on the energy of the doubly occupied orbital in d² [(Cp^R)₂Zr(CO)₂] and the singly occupied orbital in d¹ [(Cp^R)₂ZrCl₂]⁻. Since it is generally accepted that the olefin

polymerization catalysts based on alkyl zirconocenium cations are Zr^{IV} and hence d⁰, it is not yet clear how the electron-donating or -withdrawing properties of the cyclopentadienyl ligand system will effect such parameters as polymerization activity, molecular weight and stereochemistry. Future studies will extend the spectroscopic and electrochemical studies reported here to delineate how substituents influence reactivity, and specifically that related to the application of zirconocene complexes as olefin polymerization catalysts.

Experimental Section

General Considerations. All manipulations were performed using a combination of glovebox, high vacuum, and Schlenk techniques under a nitrogen or argon atmosphere. Solvents were purified and degassed by standard procedures. ¹H and ¹³C NMR spectra were measured on Varian VXR 200, 300, and 400 spectrometers and a Bruker 500 spectrometer. Chemical shifts are reported in ppm relative to SiMe₄ (δ = 0) and were referenced internally with respect to the protio solvent impurity (δ = 7.15 for C₆D₅H) and the ¹³C resonances (δ = 128.0 for C₆D₆). Coupling constants are given in hertz. IR spectra were recorded in pentane on a Perkin-Elmer Paragon 1000 spectrophotometer, and the data are reported in reciprocal centimeters. H₂C(C₅H₅)₂ was obtained by the reaction of NaCp and CH₂Br₂ according to the literature method.⁹¹ (Cp^R)₂ZrCl₂ and (Cp^R)₂Zr(CO)₂ derivatives, other than those reported below, were either obtained commercially or by literature methods.

Synthesis of [H₂C(C₅H₄)₂]ZrCl₂. A slurry of [H₂C(C₅H₄)₂]Li₂⁹² (6.00 g, 38.4 mmol) in Et₂O (150 mL) at -78 °C was added to a slurry of ZrCl₄ (8.96 g, 38.4 mmol) in Et₂O (150 mL) at -78 °C. The mixture was stirred as it was allowed to warm to room temperature and stirred for 5 days giving a yellow slurry. The volatile components were removed in vacuo, and the subsequent procedure was performed in air. The residue was extracted into CH₂Cl₂ (500 mL), after which the extract was concentrated to ca. 15 mL and treated with pentane to precipitate crude [H₂C(C₅H₄)₂]ZrCl₂. The latter material was purified by extraction into toluene followed by precipitation using pentane, giving [H₂C(C₅H₄)₂]ZrCl₂ as a bright yellow powder (2.02 g, 17%). ¹H NMR (C₆D₆): 2.95 [s, CH₂], 5.01 [t, J = 2.6, 4H of 2 C₅H₄], 6.09

(91) Schaltegger, H.; Neuenschwander, M.; Meuche, D. *Helv. Chim. Acta* **1965**, *48*, 955–961.

(92) [H₂C(C₅H₄)₂]Li₂ was obtained as a manilla powder following deprotonation of H₂C(C₅H₅)₂ with BuⁿLi in pentane/hexane.

[t , $J = 2.6$, 4H of 2 C₅H₄]. Crystals suitable for X-ray diffraction were obtained from benzene.

Synthesis of [H₂C(C₅H₄)₂]ZrCl₂. A mixture of [H₂C(C₅H₄)₂]ZrCl₂ (80 mg, 0.26 mmol) and Me₃SiI (150 μL, 1.05 mmol) in C₆H₆ (15 mL) was stirred for 3 h at room temperature. After this period, the volatile components were removed in vacuo to give [H₂C(C₅H₄)₂]ZrI₂. ¹H NMR (C₆D₆): 2.59 [s, CH₂], 4.82 [t , $J = 2.5$ Hz, 4H of 2 C₅H₄], 6.66 [t , $J = 2.5$ Hz, 4H of 2 C₅H₄]. Crystals suitable for X-ray diffraction were obtained from benzene.

Synthesis of [(C₂H₄)(C₅H₄)₂]ZrCl₂. A solution of freshly cracked CpH (41.2 mL, 0.50 mol) in THF (75 mL) was added slowly to a suspension of NaH (12.63 g, 0.50 mol) in THF (200 mL) at -78 °C. The mixture was allowed to warm to room temperature and was stirred for 30 min. After this period, the reaction mixture was cooled to -78 °C and 1,2-dibromoethane (19.4 mL, 0.225 mol) was added. The mixture was refluxed under argon for 3 h, after which water (300 mL) and pentane (500 mL) were added. The layers were separated, and the volatile components were removed from the organic layer to yield 1,2-dicyclopentadienyl ethane as a clear yellow oil (14.64 g, 41%). The 1,2-dicyclopentadienyl ethane was dissolved in pentane (200 mL), cooled to -78 °C, and treated with BuⁿLi (85 mL, 2.5M in hexanes, 0.185 mol). The mixture was allowed to warm to room temperature and stirred for 16 h and filtered. The precipitate was washed with pentane and dried in vacuo to yield [C₂H₄(C₅H₄)₂]Li₂ (7.88 g, 21%) as an off-white powder. [C₂H₄(C₅H₄)₂]Li₂ (2.00 g, 11.76 mmol) and ZrCl₄ (2.74 g, 11.76 mmol) were placed in an ampule and intimately dry-mixed. The ampule was placed at -78 °C and toluene (200 mL) was added. The mixture was allowed to warm to room temperature and stirred for 48 h. The mixture was then heated at 80 °C for 24 h and 120 °C for a further 48 h. After this period, the volatile components were removed and the residue was dissolved in CH₂Cl₂. The mixture was filtered and the filtrate was concentrated to ca. 10 mL. Addition of pentane precipitated [(C₂H₄)(C₅H₄)₂]ZrCl₂ as a white powder that was dried in vacuo after filtration (0.80 g, 21%). ¹H NMR (C₆D₆): 2.20 [s, C₂H₄], 5.44 [t , $J = 2.6$, 4H of 2 C₅H₄], 6.49 [t , $J = 2.6$, 4H of 2 C₅H₄]. Crystals suitable for X-ray diffraction were obtained from benzene.

Electrochemical Studies. Cyclic voltammetric measurements were carried out in a three-electrode cell using the BAS (Bioanalytical Systems Inc, West Lafayette, IN) potentiostat, model CV-50 W Voltammetric Analyzer, equipped with version 2.0 of the BAS CV-50 W software. A platinum disk electrode (electrode disk diameter = 1.6 mm) was used as the working electrode and a platinum wire was used as the secondary electrode. A Ag⁺/Ag reference electrode (consisting of a silver wire in acetonitrile solution containing 0.01 M AgNO₃ and 0.1 M [Buⁿ₄N][PF₆]) was used. All electrodes were obtained from BAS. The handling of solid materials was performed in an argon-filled drybox. THF (10 mL) was syringed into the electrochemical cell containing a mixture of (Cp^R)₂ZrCl₂, Cp₂Fe (internal standard), and [Buⁿ₄N][PF₆] as supporting electrolyte, to give concentrations of 10⁻³, 10⁻³, and 10⁻¹ M, respectively. Electrochemical grade [Buⁿ₄N][PF₆] was obtained from Fluka and used without further purification. THF was obtained from Fisher Chemicals and dried by refluxing over sodium in the presence of benzophenone. The cyclic voltammetric experiments were carried out under an atmosphere of argon at -41 °C by the use of an acetonitrile/liquid nitrogen slush bath. Under these conditions, the reduction potential for [Cp₂Fe]⁺/Cp₂Fe is 0.213 V relative to Ag⁺/Ag, and that for Cp₂ZrCl₂/[Cp₂ZrCl₂]⁻ is -2.040 V relative to Ag⁺/Ag (i.e., -2.253 V relative to [Cp₂Fe]⁺/Cp₂Fe). E°_{rel} values of (Cp^R)₂ZrCl₂ are quoted relative to Cp₂ZrCl₂ being equal to 0 mV.

X-ray Structure Determinations. X-ray diffraction data were collected on a Bruker P4 diffractometer equipped with a SMART CCD detector and crystal data, data collection and refinement parameters are summarized in Table 10. The structures were solved using direct methods and standard difference map techniques, and were refined by

full-matrix least-squares procedures on F^2 with SHELXTL (Version 5.03).⁹³ Hydrogen atoms on carbon were included in calculated positions.

Computational Methods. Density functional calculations were performed using the Amsterdam Density Functional code (version ADF2000.02).⁹⁴ The generalized gradient approximation was employed, using the local density approximation of Vosko, Wilk and Nusair⁹⁵ together with nonlocal exchange correction by Becke⁹⁶ and nonlocal correlation corrections by Perdew.^{97,98} Type IV basis sets were used with triple- ζ accuracy sets of Slater type orbitals, with a single polarization function added to the main group atoms. The cores of the atoms were frozen up to 1s for C and O, 2p for Si and Cl, and 3d for Zr. First-order relativistic corrections were made to the core of all atoms. Relativistic corrections were made using the ZORA (zero-order relativistic approximation) formalism.

Geometries were optimized for a series of eight bis(cyclopentadienyl) zirconium dichlorides and the analogous eight dicarbonyls. For the *ansa*-bridged species and for the Cp₂Zr derivatives C_{2v} symmetry was assumed, for Cp^{*}₂ZrCl₂ there were no symmetry restraints, and in the other cases C_2 symmetry was assumed.

Electron affinities were calculated using the optimized structure for the molecule and carrying out a single-point spin-unrestricted calculation of the negative ion.

CO stretching frequencies were calculated with the cyclopentadienyl groups and their substituents frozen to save computational time. In the case of [Me₂Si(C₅H₄)₂]Zr(CO)₂ a full frequency calculation was carried out; this gave values for ν_{CO} of 1947 and 1891 cm⁻¹ compared with 1945 and 1890 cm⁻¹ for the restricted frequency calculation. We judged the values to be sufficiently close for the restricted calculations to give an accurate representation of the trends on substitution.

Fragment calculations were carried out to elucidate the trends in the electronic structure on an orbital basis. The fragments used were the Cp^R₂Zr unit and the (CO)₂ unit with the identical geometry to that which they have in the optimized structure of the molecule.

Acknowledgment. We thank the U.S. Department of Energy, Office of Basic Energy Sciences (DE-FG02-93ER14339 to G.P. and DE-FG03-88ER13431 to J.E.B.) and the National Science Foundation (CHE-9807496 to J.E.B.) for support of this research. We thank Professor Jack Norton for use of his electrochemical equipment. Part of this work was carried out using the resources of the Oxford Super-Computing Centre and the EPSRC Columbus cluster at the Rutherford laboratory. We thank Professor Hans Brintzinger for a preprint of references 18b and 71d.

Supporting Information Available: Tables of crystallographic data and figures (PDF). This material is available free of charge via the Internet at <http://pubs.acs.org>.

JA020236Y

- (93) Sheldrick, G. M. SHELXTL, An Integrated System for Solving, Refining and Displaying Crystal Structures from Diffraction Data; University of Göttingen, Göttingen, Federal Republic of Germany, 1981.
- (94) ADF Program System Release 2000.02, Baerends, E. J.; Bérces, A.; Bo, C.; Boerigter, P. M.; Cavallo, L.; Deng, L.; Dickson, R. M.; Ellis, D. E.; Fan, L.; Fischer, T. H.; Fonseca Guerra, C.; van Gisbergen, S. J. A.; Groeneveld, J. A.; Gritsenko, O. V.; Harris, F. E.; van den Hoek, P.; Jacobsen, H.; van Kessel, G.; Kootstra, F.; van Lenthe, E.; Osinga, V. P.; Philipsen, P. H. T.; Post, D.; Pye, C. C.; Ravenek, W.; Ros, P.; Schipper, P. R. T.; Schreckenbach, G.; Snijders, J. G.; Sola, M.; Swerhone, D.; te Velde, G.; Vernooijs, P.; Versluis, L.; Visser, O.; van Wezenbeek, E.; Wiesenekker, G.; Wolff, S. K.; Woo, T. K.; Ziegler, T. Free University, Amsterdam, 2000.
- (95) Vosko, S. H.; Wilk, L.; Nusair, M. *Can. J. Phys.* **1980**, *58*, 1200–1211.
- (96) Becke, A. D. *Phys. Rev. A* **1988**, *38*, 3098–3100.
- (97) Perdew, J. P. *Phys. Rev. B* **1986**, *33*, 8822–8824.
- (98) Perdew, J. P. *Phys. Rev. B* **1986**, *34*, 7046.